A general Fourier expansion of post-Newtonian binary dynamics based on quasi-Keplerian framework

Xiaolin Liu[1,*] and Zhoujian Cao[†2,3,4,2,‡]

[1]*Instituto de Física Téorica UAM-CSIC, Universidad Autónoma de Madrid, Cantoblanco 28049 Madrid, Spain*
[2]*Institute for Frontiers in Astronomy and Astrophysics, Beijing Normal University, Beijing 102206, China*
[3]*Department of Astronomy, Beijing Normal University, Beijing 100875, China*
[4]*School of Fundamental Physics and Mathematical Sciences, Hangzhou Institute for Advanced Study, UCAS, Hangzhou 310024, China*

We have introduced a new Fourier-expansion technique for computing gravitational-wave emission from non-spinning binaries in the post-Newtonian framework. Using this approach, we derived the full set of 3PN dynamical quantities and gravitational-wave Fourier modes and have released the corresponding numerical code as open source. Furthermore, applying the method to the tail contribution of the energy flux, we found that it can be resummed into an exceptionally compact expression. These advances pave the way for more convenient and accurate frequency-domain waveform modeling in the future.

I. INTRODUCTION

Since the first observation in 2015 [1], gravitational-wave (GW) astronomy has advanced rapidly. Joint observing runs by LIGO, Virgo, and KAGRA [2–4] have amassed a rich data set [5, 6], and—using techniques such as matched filtering against theoretical templates—researchers have identified scores of binary-black-hole (BBH), binary-neutron-star (BNS), and even black-hole–neutron-star (NSBH) merger events. More recently, pulsar-timing-array (PTA) experiments have reported evidence for a stochastic background produced by super-massive binary-black-hole mergers [7–10]. Looking ahead, next-generation ground-based detectors like the Einstein Telescope (ET) [11] and Cosmic Explorer (CE) [12], together with planned space missions such as LISA [13], TianQin [14], Taiji [15], and DECIGO [16], are expected to uncover many more GW signals.

The dominant sources of GWs in the Universe are generally compact binaries. The background generated by systems such as BBHs is thought to prevail over a wide range of frequencies [17]. Current data-analysis pipelines—whether based on traditional matched filtering or modern machine-learning methods—depend [18] critically on accurate models of two-body dynamics and GW emission in general relativity. Numerical-relativity (NR) simulations have already produced extensive catalogs of binary waveforms, greatly aiding model development [19–21]. Nevertheless, their high computational cost limits waveform length, a constraint that becomes severe as future detectors push to lower frequencies. At the other extreme, the self-force framework treats motion in a known black-hole spacetime as a perturbative expansion in a small mass ratio, yielding precise geodesic orbits and, via perturbation theory, far-zone waveforms [22, 23]. Together, NR and self-force methods offer solutions in the strong-field comparable-mass and large-mass-ratio regimes, respectively.

For weak-field, slow-motion systems, the post-Newtonian–Multipolar-post-Minkowskian (PN–MPM) expansion provides an analytic framework [24]: the field equations are recast as nonlinear wave equations on a flat background, and formal solutions emerge through multipolar expansions. PN theory has seen substantial progress, underpinning mainstream waveform models such as effective-one-body (EOB) [25] models, including SEOBNR models [26–31], TEOBResum models [32–34] and IMR families [35–41]. Current ground-based detectors are sensitive to higher-frequency bands, which typically correspond to the late-stage evolution of binaries approaching circular orbits. In contrast, future low-frequency detectors will be more concerned with binaries exhibiting non-zero eccentricities. Moreover, in recent years, GW events with possible residual eccentricities have been identified [42], which has driven the development of gravitational wave models that incorporate eccentricity.

However, when we look ahead to future low-frequency detectors, constructing accurate frequency-domain GW models for generic orbits remains a difficult task. The standard strategy is to express the post-Newtonian (PN) orbit in a quasi-Keplerian parametrization [43–46] and then compute its evolution using an adiabatic approximation or a

† corresponding author
*Xiaolin Liu: `shallyn.liu@foxmail.com`
‡Zhoujian Cao: `zjcao@amt.ac.cn`

multi-scale expansion [47, 48]. Waveform generation, in turn, relies on analytic Fourier-transform techniques—such as the stationary-phase approximation (SPA) [49] for non-precessing binaries and the shift-uniform approximation (SUA) [50] when spin precession is present. Unfortunately, these frequency-domain waveforms all depend on a small-eccentricity expansion, which tends to break down at large eccentricities.

Recent work has shown that by keeping the Bessel functions that naturally appear in the original Fourier modes of the gravitational radiation, one can avoid the accuracy loss at high eccentricity caused by the small-eccentricity expansion [51]. This insight suggests that we need to investigate more deeply the structure of the Fourier modes of both the dynamics and the radiative multipole moments within the PN framework. Building on the studies of [52] and [51, 53], we therefore propose a mathematical approach for describing and computing the Fourier modes of the dynamics and waveforms of a PN two-body system, and we revisit the theoretical treatment of nonlinear contributions. All implementation code is available in the open-source library `pyPNFourier`.

II. THEORETICAL BACKGROUND AND REVIEW

A. Post-Newtonian Dynamical System and the Quasi-Keplerian Parameterization

The post-Newtonian approximation solves the Einstein field equations perturbatively in the weak-field, slow-motion regime [24, 54]. For a two-body system, the equations of motion can be expanded as a power series in c^{-1}. Neglecting spin and radiation-reaction effects, the acceleration is now known through 4 PN order [55, 56],

$$\boldsymbol{a} = \boldsymbol{a}_N + \frac{1}{c^2}\boldsymbol{a}_{1\text{PN}} + \frac{1}{c^4}\boldsymbol{a}_{2\text{PN}} + \frac{1}{c^6}\boldsymbol{a}_{3\text{PN}} + \frac{1}{c^6}\big(\boldsymbol{a}_{4\text{PN}} + \boldsymbol{a}_{\text{tail}}\big) + \mathcal{O}\big(c^{-5}\big), \tag{1}$$

where the 4PN tail term $\boldsymbol{a}_{\text{tail}}$ represents the back-reaction on the binary from the multipolar GW flux and is a manifestation of the non-linearity of general relativity [55, 57, 58]. When this non-linear effect is ignored, the system can be described by the two conserved quantities, the energy E and the angular momentum J. Starting at 2PN order the field integrals become divergent; to cure this one introduces Hadamard finite-part regularization [59] and dimensional regularizatioin, which in turn brings in logarithmic terms and an arbitrary length scale r_0. A modified harmonic (MH) coordinate system is therefore defined to eliminate the logarithms [60, 61]; we adopt MH coordinates throughout this work.

The PN two-body problem corresponds to a precessing elliptical orbit that can still be described in terms of the familiar orbital elements such as the eccentricity e and semi-major axis a. This is the essence of the quasi-Keplerian parameterization [43–46], widely used in contemporary waveform models (e.g. the PN models [62–65], IMR family [40, 41] and the latest EOB model [30]). The 4PN results of instantaneous part was found in ADM coordinates[66]; here we use MH coordinates and, for completeness, list in the Appendix the 4PN transformations among the MH, SH, EOB [67–69], and ADM frames.

We now briefly review the method and the results needed below, following [46]. The radial velocity $\dot{r}$ can be written as a function of (E, J, u) with $u := 1/r$. Solving $\dot{r}(E, J, u) = 0$ yields two roots $u_\pm$ corresponding to periastron and apastron, from which we define the semi-major axis and (radial) eccentricity e_r

$$a_r := \frac{u_+ + u_-}{2u_+u_-}, \qquad e_r := \frac{u_- - u_+}{u_- + u_+}. \tag{2}$$

The orbital period P is twice the travel time from u_- to u_+. Since u varies between these bounds we introduce two auxilary angles χ, ζ

$$u = \frac{1 + e_r\cos\zeta}{a_r(1 - e_r^2)} = \frac{1}{a_r\big(1 - e_r\cos\chi\big)}, \tag{3}$$

where ζ is the relativistic anomaly and χ the eccentric anomaly. The third angle, called true anomaly ψ, is defined by

$$\psi := 2\arctan\left(\left(\frac{1+e_\phi}{1-e_\phi}\right)^{1/2}\tan\frac{\chi}{2}\right) = 2\arctan\left(\left(\frac{1+e_r}{1-e_r}\right)^{1/2}\tan\frac{\zeta}{2}\right), \tag{4}$$

and introducing a new eccentricity e_ϕ. Owing to later naming conflicts we employ a convention that differs from many references. The mean anomaly $l := n(t - t_0)$ with $n := 2\pi/P$, is related to χ by the Kepler equation; up to 4PN it takes the form

$$l = \chi - e_t\sin\chi + \left(\frac{1}{c^4}g_{4t} + \frac{1}{c^6}g_{6t} + \frac{1}{c^8}g_{8t}\right)(\psi - \chi) + \left(\frac{1}{c^4}f_{4t} + \frac{1}{c^6}f_{6t} + \frac{1}{c^8}f_{8t}\right)\sin\psi + \left(\frac{1}{c^6}i_{6t} + \frac{1}{c^8}i_{8t}\right)\sin 2\psi$$

$$+\left(\frac{1}{c^6}h_{6t}+\frac{1}{c^8}h_{8t}\right)\sin 3\psi+\frac{1}{c^8}j_{8t}\sin 4\psi+\mathcal{O}\left(c^{-10}\right), \tag{5}$$

where the leading-order coefficient of $\sin\chi$ is the time eccentricity e_t, the eccentricity used by most models. Unless stated otherwise we henceforth drop the subscript and write e.

We next introduce

$$x:=\omega^{2/3}, \qquad \omega:=(1+k)n, \tag{6}$$

where k is the periastron advance defined via the orbital phase ϕ accumulated in one radial period,

$$1+k:=\frac{1}{2\pi}\left(-\int_{u_+}^{u_-}\frac{\mathrm{d}\phi}{\mathrm{d}u}\,\mathrm{d}u\right). \tag{7}$$

For convenience we later set $v:=x^{1/2}$. With these relations (E,J) can be expressed in terms of (x,e), and the basic dynamical variables $(r,\dot{r},\phi,\dot{\phi})$ in terms of (x,e,χ). Of particular interest is the orbital phase,

$$\phi=\lambda+W(v,e;l), \qquad \lambda:=(1+k)l \;\;\Rightarrow\;\; \dot{\lambda}=\omega, \tag{8}$$

where

$$W(v,e;l)=\chi_t-\chi+e\sin\chi+\mathcal{O}\left(c^{-2}\right), \qquad \chi_t:=2\arctan\left(\left(\frac{1+e}{1-e}\right)^{1/2}\tan\frac{\chi}{2}\right). \tag{9}$$

Defining $\delta\chi:=\chi_t-\chi=2\arctan\left(\beta_e\sin\chi/\left(1-\beta_e\cos\chi\right)\right)$ with

$$\beta_e:=\frac{1-\sqrt{1-e^2}}{e}. \tag{10}$$

We express ψ in terms of χ_t in the following sections. One can perform the needed Fourier transformations following [70]. All 4PN quasi-Keplerian parameterization results are collected in the Supplementary Material.

B. General Method for Gravitational-Wave Calculations

In the PN-MPM framework [71, 72], the GW polarizations $h_{+,\times}$ measured by a distant observer depend on the radiative multipoles (U_L,V_L), which in turn depend on the source multipoles $(I_L,J_L,\dots)$ and non-linear hereditary terms [73]. All are ultimately functions of the source dynamics, schematically $h(v,e;l)$. Within the QK framework one solves for the adiabatic evolution of (v,e,l) under radiation reaction. After averaging over one radial period (the adiabatic or orbital average) one obtains $(\bar{v},\bar{e},\bar{l})$ from the energy and angular-momentum fluxes at infinity,

$$\langle\dot{\bar{v}}\rangle=\frac{\partial v}{\partial E}\langle\mathcal{F}\rangle+\frac{\partial v}{\partial J}\langle\mathcal{G}\rangle, \tag{11}$$

$$\langle\dot{\bar{e}}\rangle=\frac{\partial e}{\partial E}\langle\mathcal{F}\rangle+\frac{\partial e}{\partial J}\langle\mathcal{G}\rangle, \tag{12}$$

where the orbital average $\langle\cdot\rangle$ denotes

$$\langle f\rangle:=\frac{1}{2\pi}\int_0^{2\pi}f(l)\mathrm{d}l. \tag{13}$$

The fluxes $\mathcal{F}$ and $\mathcal{G}$ are computed from the radiative multipoles; their difference from the actual loss of the system energy E and angular J is the Schott term [74], which vanishes upon orbital averaging for 2.5PN, 3.5PN and 4.5PN and doesn't vanish for 4PN due to the hereditary effect**??**, leaving some freedom in the explicit form of the radiation-reaction force [75]. The radiation-reaction force of non-spinning binary is known up to 4.5PN [76–79]. Multiscale analysis then yields post-adiabatic corrections [47, 48]. For current 3PN waveform models only the first-order correction $(\tilde{v},\tilde{e},\tilde{l})$ is required [80], which can be evaluated from $(\bar{v},\bar{e},\bar{l})$ and substituted into $h(v,e;l)$.

Because data analysis is performed mainly in the frequency domain, analytic Fourier approximations are highly desirable—especially for future low-frequency GW detectors. In the non-spinning case one expands

$$h=\sum_{m,p}\tilde{h}_{mp}(v,e)\mathrm{e}^{\mathrm{i}(m\lambda+pl)}, \tag{14}$$

and applies the stationary-phase approximation (SPA) to each mode [49], expanding the phase

$$\phi_{mp}(t) = m\lambda + pl - 2\pi f t \tag{15}$$

about the SPA time t_{mp} as

$$\phi_{mp}(t) \approx \phi_{mp}(t_{mp}) + (t - t_{mp})\dot{\phi}_{mp}(t_{mp}) + \frac{1}{2}(t - t_{mp})^2 \ddot{\phi}_{mp}, \tag{16}$$

with the condition

$$\dot{\phi}_{mp} = 0 \implies m\omega(t_{mp}) + pn(t_{mp}) = 2\pi f := v_f^3. \tag{17}$$

For non-spinning case one could assume the amplitude of the mode grows much slower than phase. However this do not hold for spin-precessing is included, where the Shifted Uniform Asymptotics (SUA) method is applied [65].

Since post-adiabatic effects enter at v^5, one first solves for the averaged part, giving $\bar{v}^3 = (m+p)^{-1} v_f^3 \big(1 + \mathcal{O}(\bar{v})\big)$, and then substitutes v_f for $\bar{v}$ in the corrections $(\tilde{v}, \tilde{e}, \tilde{l}, \dots)$.

In principle there is no closed-form relation between $\bar{v}$, $\bar{l}$, and $\bar{e}$. One strategy is to expand $\bar{e}$ around its initial value e_0, but high initial eccentricity requires very high expansion order. Padé resummation has been introduced to improve accuracy in that regime [81]. Recent work shows that one can directly integrate numerically with a standard Runge–Kutta scheme [51], using $\bar{v}$ rather than t as the independent variable, and then determine t_{mp} by interpolation from the relation $\bar{v}^3 = (m+p)^{-1} v_f^3 \big(1 + \mathcal{O}(\bar{v})\big)$. Given f and (p, m), this yields the averaged orbital frequency $\bar{v}(t_{mp})$ and all other dynamical quantities.

III. FOURIER SERIES OF BOUNDED-BINARY PN DYNAMICS

[52] showed that, at Newtonian order, the Fourier modes of a binary system's multipole moments can be expressed in terms of Bessel functions. Because the gravitational field is sourced by these radiative multipole moments, its Fourier modes inherit the same structure. Recent studies[51, 53] have demonstrated that this property can be exploited to compute arbitrary Fourier modes rapidly, thereby greatly improving the accuracy of eccentric-orbit models. However, at higher PN orders ordinary Bessel functions are no longer sufficient; here we introduce a new family of generalized, Bessel-like elliptic integrals that can represent the Fourier modes of all post-Newtonian multipole moments.

A. Generalized Bessel elliptical function

The non-spinning binary's dynamics in the PN framework is characterized by a double periodicity. The Fourier series of a dynamical quantity f takes the form

$$f(\lambda, \chi) = \sum_{p,m=-\infty}^{\infty} \hat{f}^{(p,m)} \mathrm{e}^{\mathrm{i}(p\ell + m\lambda)}, \tag{18}$$

where the Fourier coefficient $\hat{f}^{(p,m)}$ is given by

$$\hat{f}^{(p,m)} = \frac{1}{(2\pi)^2} \iint_{-\pi}^{\pi} f(\lambda, \chi) \mathrm{e}^{-\mathrm{i}(p\ell + m\lambda)} \, \mathrm{d}\ell \, \mathrm{d}\lambda \,. \tag{19}$$

Here we use χ is because In most cases the quantity depends on χ rather than l. And usually, the dependence on λ mainly comes from the orbital phase $\phi = \lambda + W(l)$, so we can simplify it via

$$f(\lambda, \chi) = \sum_{m=-\infty}^{\infty} f^m(\chi) \mathrm{e}^{\mathrm{i}m\lambda}, \tag{20}$$

$$\begin{aligned}
\hat{f}^{(p,m)} &= \frac{1}{2\pi} \int_{-\pi}^{\pi} f^{(m)}(\chi) \mathrm{e}^{-\mathrm{i}p\ell} \, \mathrm{d}\ell \\
&= \frac{1}{2\pi} \int_{-\pi}^{\pi} f^{(m)}(\chi) \frac{\mathrm{d}\ell}{\mathrm{d}\chi} \, \mathrm{d}\chi
\end{aligned} \tag{21}$$

One would find that after sorting, up to 3PN order, these Fourier coefficients can be expressed by two kinds of integrals,

$$\mathrm{J}^{(n)}_{pqa}(e) := \frac{1}{2\pi}\int_{-\pi}^{\pi}\frac{\mathrm{e}^{\mathrm{i}(p\chi - qe\sin\chi)}}{(1-e\cos\chi)^a}(\mathrm{i}\delta\chi)^n\mathrm{d}\chi, \tag{22}$$

$$\mathrm{K}^{(n)}_{pqa}(e) := \frac{1}{2\pi}\int_{-\pi}^{\pi}\frac{\mathrm{e}^{\mathrm{i}(p\chi - qe\sin\chi)}}{(1-e\cos\chi)^a}(\mathrm{i}\delta\chi)^c\ln(1-e\cos\chi)\mathrm{d}\chi, \tag{23}$$

These integrals can be viewed as extensions of Bessel functions or Hansen coefficients [82]. And also can be regarded as the extension of [83–85]. For example, $\mathrm{J}^{(0)}_{pq0} \equiv J_p(qe)$. The factor $(1-e\cos\chi)$ shows in the denominator can be regarded as the derivative with respect to l, since

$$\frac{\mathrm{d}f}{\mathrm{d}l} = \frac{\mathrm{d}f}{\mathrm{d}\chi}\frac{\mathrm{d}\chi}{\mathrm{d}l} = \frac{1}{1-e\cos\chi}\frac{\mathrm{d}f}{\mathrm{d}\chi} + \mathcal{O}\big(c^{-4}\big). \tag{24}$$

At 3PN order, we only encounter the term $\mathrm{J}^{(3)}_{pqa}$ and $\mathrm{K}^{(0)}_{pqa}$. By observing the symmetry of the integrands we can quickly obtain some properties,

$$\mathrm{J}^{(n)}_{(-p)(-q)a} = (-1)^n\mathrm{J}^{(n)}_{pqa},\ \mathrm{K}^{(n)}_{(-p)(-q)a} = \mathrm{K}^{(n)}_{pqa}. \tag{25}$$

And the properties of differentiation,

$$\frac{\partial}{\partial e}\mathrm{J}^{(n)}_{pqa} = \frac{q}{2}\Big(\mathrm{J}^{(n)}_{(p-1)qa} - \mathrm{J}^{(n)}_{(p+1)qa}\Big) + \frac{a}{2}\Big(\mathrm{J}^{(n)}_{(p-1)q(a+1)} + \mathrm{J}^{(n)}_{(p+1)q(a+1)}\Big) - \frac{n}{2\sqrt{1-e^2}}\Big(\mathrm{J}^{(n-1)}_{(p-1)q(a+1)} - \mathrm{J}^{(n-1)}_{(p+1)q(a+1)}\Big), \tag{26}$$

$$\begin{aligned}\frac{\partial}{\partial e}\mathrm{K}^{(n)}_{pqa} = {}& \frac{q}{2}\Big(\mathrm{K}^{(n)}_{(p-1)qa} - \mathrm{K}^{(n)}_{(p+1)qa}\Big) + \frac{a}{2}\Big(\mathrm{K}^{(n)}_{(p-1)q(a+1)} + \mathrm{K}^{(n)}_{(p+1)q(a+1)}\Big) - \frac{n}{2\sqrt{1-e^2}}\Big(\mathrm{K}^{(n-1)}_{(p-1)q(a+1)} - \mathrm{K}^{(n-1)}_{(p+1)q(a+1)}\Big)\\ &- \frac{1}{2}\Big(\mathrm{K}^{(n)}_{(p-1)q(a+1)} + \mathrm{K}^{(n)}_{(p+1)q(a+1)}\Big),\end{aligned} \tag{27}$$

And recursion identities

$$2p\mathrm{J}^{(n)}_{pqa} = e\bigg[q\Big(\mathrm{J}^{(n)}_{(p+1)qa} + \mathrm{J}^{(n)}_{(p-1)qa}\Big) + a\Big(\mathrm{J}^{(n)}_{(p-1)q(a+1)} - \mathrm{J}^{(n)}_{(p+1)q(a+1)}\Big)\bigg] + \frac{2n\beta_e(1-\beta_e)}{1+\beta_e^2}\Big(\mathrm{J}^{(n+1)}_{(p-1)q(a+1)} + \mathrm{J}^{(n+1)}_{(p+1)q(a+1)}\Big), \tag{28}$$

$$\begin{aligned}2p\mathrm{K}^{(n)}_{pqa} = {}& e\Big(\mathrm{J}^{(n)}_{(p-1)q(a+1)} - \mathrm{J}^{(n)}_{(p+1)q(a+1)}\Big) + e\bigg[q\Big(\mathrm{K}^{(n)}_{(p+1)qa} + \mathrm{K}^{(n)}_{(p-1)qa}\Big) + a\Big(\mathrm{K}^{(n)}_{(p-1)q(a+1)} - \mathrm{K}^{(n)}_{(p+1)q(a+1)}\Big)\bigg]\\ &+ \frac{2n\beta_e(1-\beta_e)}{1+\beta_e^2}\Big(\mathrm{K}^{(n+1)}_{(p-1)q(a+1)} + \mathrm{K}^{(n+1)}_{(p+1)q(a+1)}\Big),\end{aligned} \tag{29}$$

$$\mathrm{J}^{(n)}_{pq(a-1)} = \mathrm{J}^{(n)}_{pqa} + \frac{e}{2}\Big(\mathrm{J}^{(n)}_{(p+1)qa} + \mathrm{J}^{(n)}_{(p-1)qa}\Big),\ \mathrm{K}^{(n)}_{pq(a-1)} = \mathrm{K}^{(n)}_{pqa} + \frac{e}{2}\Big(\mathrm{K}^{(n)}_{(p+1)qa} + \mathrm{K}^{(n)}_{(p-1)qa}\Big), \tag{30}$$

$$\frac{e}{2}\Big(\mathrm{J}^{(n)}_{(p+1)qa} - \mathrm{J}^{(n)}_{(p-1)qa}\Big) = \frac{1}{1-a}\bigg(p\mathrm{J}^{(n)}_{pq(a-1)} + q\Big(\mathrm{J}^{(n)}_{pq(a-2)} - \mathrm{J}^{(n)}_{pq(a-1)}\Big) + n\sqrt{1-e^2}\mathrm{J}^{(n-1)}_{pqa}\bigg), \tag{31}$$

$$\begin{aligned}\frac{e}{2}\Big(\mathrm{K}^{(n)}_{(p+1)qa} - \mathrm{K}^{(n)}_{(p-1)qa}\Big) = {}& \frac{1}{1-a}\bigg(p\mathrm{K}^{(n)}_{pq(a-1)} + q\Big(\mathrm{K}^{(n)}_{pq(a-2)} - \mathrm{K}^{(n)}_{pq(a-1)}\Big) + n\sqrt{1-e^2}\mathrm{K}^{(n-1)}_{pqa}\\ &- \frac{e^2}{2}\Big(\mathrm{J}^{(n)}_{(p+1)qa} - \mathrm{J}^{(n)}_{(p-1)qa}\Big)\bigg)\end{aligned} \tag{32}$$

At some special cases, we have [86],

$$\mathrm{J}^{(0)}_{00a} = \frac{1}{(1-e^2)^{a/2}}P_{a-1}\Big(\frac{1}{\sqrt{1-e^2}}\Big), \tag{33}$$

$$\mathrm{K}^{(0)}_{00a} = \frac{(-1)^{a-1}}{(a-1)!}\Big(\frac{\mathrm{d}^{a-1}Y(y,e)}{\mathrm{d}y^{a-1}}\Big)_{y=1}, \tag{34}$$

$$\mathrm{K}^{(0)}_{p00} = -\frac{\beta_e^{|p|}}{|p|}. \tag{35}$$

where $P_N(x)$ is Legendre polynomial and

$$Y(y,e) = \frac{1}{\sqrt{y^2-e^2}}\Big[\ln\Big(\frac{\sqrt{1-e^2}+1}{2}\Big) + 2\ln\Big(1+\frac{\sqrt{1-e^2}-1}{y+\sqrt{y^2-e^2}}\Big)\Big]. \tag{36}$$

These integrals generally do not have a closed form, but they can be easily expanded as power series of eccentricity. We reorganize them into the infinite series of Bessel function and β_e,

$$\mathrm{J}^{(0)}_{pqa} = (1+\beta_e^2)^a \sum_{k=-\infty}^{\infty} (-1)^k J_k(qe)\mathcal{L}^{(a)}_{k+p}, \tag{37}$$

$$\mathrm{J}^{(1)}_{pqa} = (1+\beta_e^2)^a \sum_{n=0}^{\infty}\sum_{\delta=\pm1} \frac{\delta\beta_e^{n+1}}{n+1} \sum_{k=-\infty}^{\infty} (-1)^k J_k(qe)\mathcal{L}^{(a)}_{k+p+\delta(n+1)}, \tag{38}$$

$$\mathrm{J}^{(2)}_{pqa} = -(1+\beta_e^2)^a \sum_{n=0}^{\infty}\sum_{s=0}^{n}\sum_{\delta=\pm1} \frac{\beta_e^{n+2}}{(s+1)(n-s+1)} \sum_{k=-\infty}^{\infty} (-1)^k J_k(qe)\big(\mathcal{L}^{(a)}_{k+p+\delta(n-2s)} - \mathcal{L}^{(a)}_{k+p+\delta(n+2)}\big), \tag{39}$$

$$\begin{aligned}\mathrm{J}^{(3)}_{pqa} = -(1+\beta_e^2)^a &\sum_{n=0}^{\infty}\sum_{s_1=0}^{n}\sum_{s_2=0}^{s_1}\sum_{\delta=\pm1} \frac{\delta\beta_e^{n+3}}{(s_1-s_2+1)(n-s_1+1)(s_2+1)} \\ &\times \sum_{k=-\infty}^{\infty} (-1)^k J_k(qe)\big(\mathcal{L}^{(a)}_{k+p+\delta(1+n-2s_2)} + \mathcal{L}^{(a)}_{k+p+\delta(1+n-2s_1+2s_2)} - \mathcal{L}^{(a)}_{k+p+\delta(n+3)} - \mathcal{L}^{(a)}_{k+p+\delta(n-1-2s_1)}\big),\end{aligned} \tag{40}$$

$$\mathrm{K}^{(0)}_{pqa} = -(1+\beta_e^2)^a \sum_{k=-\infty}^{\infty} (-1)^k J_k(qe)\Big(\mathcal{L}^{(a)}_{k+p}\ln\big(1+\beta_e^2\big) + \frac{\mathrm{d}}{\mathrm{d}a}\mathcal{L}^{(a)}_{k+p}\Big) \tag{41}$$

where $\mathcal{L}^{(a)}_n$ denotes an extension of Laplace coefficients [87],

$$\mathcal{L}^{(a)}_n(\beta_e) := \frac{1}{2\pi}\int_{-\pi}^{\pi} \frac{\mathrm{e}^{iny}}{(1+\beta_e^2-2\beta_e\cos y)^a}\,\mathrm{d}y\,, \tag{42}$$

which is also equivalent to

$$\mathcal{L}^{(a)}_n(\beta_e) = \Big(\frac{e}{2\beta_e}\Big)^a \mathrm{J}^{(0)}_{n0a}(e). \tag{43}$$

It can be written in the form of a hypergeometric function. Since the coefficients of this hypergeometric function are non-negative, it can be further expanded into a finite polynomial of β_e when $a>0$,

$$\begin{aligned}\mathcal{L}^{(a)}_n &= \frac{(a)_{|n|}}{|n|!}\beta_e^{|n|}(1-\beta_e^2)^{1-2a}[{}_2\mathrm{F}_1]\left(\begin{matrix}1-a,\ |n|+1-a \\ |n|+1\end{matrix};\beta_e^2\right) \\ &= (a)_{|n|}\beta_e^{|n|}(1-\beta_e^2)^{1-2a}\sum_{m=0}^{a-1}\frac{(-1)^m(|n|+1-a)_m}{(|n|+m)!}\binom{a-1}{m}\beta_e^{2m},\end{aligned} \tag{44}$$

where the general hypergeometric function is defined by [88]

$$[{}_p\mathrm{F}_q]\left(\begin{matrix}a_1,a_2,...a_p \\ b_1,b_2,...b_q\end{matrix};y\right) = \sum_{m=0}^{\infty}\frac{(a_1)_m(a_2)_m...(a_p)_m}{(b_1)_m(b_2)_m...(b_q)_m}\frac{x^m}{m!}. \tag{45}$$

And $(a)_n := \Gamma(a+n)/\Gamma(a)$ is Pochhammer symbol. $\frac{\mathrm{d}}{\mathrm{d}a}\mathcal{L}^{(a)}_n$ is the formal derivative with respect to a, which takes a polynomial series,

$$\frac{\mathrm{d}}{\mathrm{d}a}\mathcal{L}^{(a)}_n := |n|!\sum_{m=0}^{\infty}\frac{1}{(|n|+m)!m!}\beta_e^{2m}\frac{\mathrm{d}}{\mathrm{d}a}\Big[(1-a)_m(|n|+1-a)_m\Big], \tag{46}$$

where the Pochhammers' derivative with respective to a is

$$\frac{\mathrm{d}}{\mathrm{d}a}(1-a)_m = \begin{cases}(1-a)_m\Delta\mathrm{H}^a_{a-m} & m\le a-1 \\ (-1)^a\Gamma(a)\Gamma(m+1-a) & m\ge a\end{cases} \tag{47}$$

$$\frac{\mathrm{d}}{\mathrm{d}a}(|n|+1-a)=\begin{cases}(|n|+1-a)_m\Delta\mathrm{H}^{|n|+1-a}_{|n|+1+m-a} & a\le n,\\ (|n|+1-a)_m\Delta\mathrm{H}^{a-|n|}_{a-m-|n|} & a\ge n+1 \text{ and } m\le a-|n|-1,\\ (-1)^{a-|n|}\Gamma(a-|n|)\Gamma(m+|n|+1-a) & a\ge n+1 \text{ and } m\ge a-|n|\end{cases}\tag{48}$$

$\Delta\mathrm{H}^n_m$ denotes the difference between the $(n-1)$th and $(m-1)$th Harmonic number. The poles produced by the di-Gamma function $\psi(x):=\Gamma'(x)/\Gamma(x)$ divided by the Gamma function are removed by the following limit,

$$\lim_{n\to\mathbb{Z}^+}\frac{\psi(1-n)}{\Gamma(1-n)}=(-1)^n(n-1)!.\tag{49}$$

Specifically, when $a=0$,

$$\frac{\mathrm{d}}{\mathrm{d}a}\,\mathcal{L}^{(a)}_n\bigg|_{a=0}=\begin{cases}\beta^{|n|}/|n| & n\neq 0\\ 0 & n=0.\end{cases}\tag{50}$$

Here we recall the Kepteyn series of standard Bessel functions [89]

$$\frac{1}{1-e}=\sum_{p=-\infty}^{\infty}\mathrm{J}^{(0)}_{pp0},\tag{51}$$

$$\frac{1}{\sqrt{1-e^2}}=\sum_{p=-\infty}^{\infty}\big(\mathrm{J}^{(0)}_{pp0}\big)^2.\tag{52}$$

These identities can be generalized to

$$\frac{\delta_{n0}}{(1-e)^{a+1}}=\sum_{p=-\infty}^{\infty}\mathrm{J}^{(n)}_{ppa},\quad \frac{\delta_{n0}\ln(1-e)}{(1-e)^{a+1}}=\sum_{p=-\infty}^{\infty}\mathrm{K}^{(n)}_{ppa},\tag{53}$$

$$\mathrm{J}^{(c+d)}_{m0(a+b)}=\sum_{p=-\infty}^{\infty}\mathrm{J}^{(c)}_{(p+m)qa}\mathrm{J}^{(d)}_{pqb},\quad \mathrm{K}^{(c+d)}_{m0(a+b)}=\sum_{p=-\infty}^{\infty}\mathrm{J}^{(c)}_{(p+m)qa}\mathrm{K}^{(d)}_{pqb},\quad \mathrm{L}^{(c+d)}_{m0(a+b)}=\sum_{p=-\infty}^{\infty}\mathrm{K}^{(c)}_{(p+m)qa}\mathrm{K}^{(d)}_{pqb},\tag{54}$$

where $\mathrm{L}^{(n)}_{pqa}$ is defined via

$$\mathrm{L}^{(n)}_{pqa}:=\frac{1}{2\pi}\int_{-\pi}^{\pi}\frac{\mathrm{e}^{\mathrm{i}(p\chi-qe\sin\chi)}}{(1-e\cos\chi)^a}\ln^2\big(1-e\cos\chi\big)(\mathrm{i}\delta\chi)^n\,\mathrm{d}\chi\,.\tag{55}$$

The proof of the first identity is easy,

$$\begin{aligned}\sum_{p=-\infty}^{\infty}\mathrm{J}^{(n)}_{ppa}&=\frac{1}{2\pi}\int_{-\pi}^{\pi}(\mathrm{i}\delta\chi)^n(1-e\cos\chi)^{-a}\sum_{p=-\infty}^{\infty}\mathrm{e}^{\mathrm{i}(p\chi-pe\sin\chi)}\mathrm{d}\chi\\ &=\int_{-\pi}^{\pi}(\mathrm{i}\delta\chi)^n(1-e\cos\chi)^{-a}\delta\big(p(\chi-e\sin\chi)\big)\mathrm{d}\chi=\frac{\delta_{n0}}{(1-e)^{a+1}},\end{aligned}\tag{56}$$

where we use the Poisson summation formula

$$\sum_{p=-\infty}^{\infty}\mathrm{e}^{\mathrm{i}px}=2\pi\sum_{k=-\infty}^{\infty}\delta(x-2\pi k).\tag{57}$$

The proof of the second identity is similar,

$$\begin{aligned}\sum_{p=-\infty}^{\infty}\mathrm{J}^{(c)}_{(p+m)qa}\mathrm{J}^{(d)}_{pqb}&=\frac{1}{(2\pi)^2}\iint_{-\pi}^{\pi}\frac{\mathrm{e}^{\mathrm{i}\left[mx-q(\sin x-\sin y)\right]}}{(1-e\cos x)^a(1-e\cos y)^b}\mathrm{i}^{c+d}\delta\chi(x)^c\delta\chi(y)^d\sum_{p=-\infty}^{\infty}\mathrm{e}^{\mathrm{i}p(x-y)}\,\mathrm{d}x\,\mathrm{d}y\,,\\ &=\frac{1}{2\pi}\int_{-\pi}^{\pi}\frac{\mathrm{e}^{\mathrm{i}mx}\,\mathrm{d}x}{(1-e\cos x)^{a+b}}\big(\mathrm{i}\delta\chi(x+y)\big)^{c+d}=\mathrm{J}^{(c+d)}_{m0(a+b)},\end{aligned}\tag{58}$$

where we use $\sum_p e^{ip(x-y)} = 2\pi\delta(x-y)$. Note that this identity is independent of q. For other cases involving logarithms, just add the logarithmic term to the integral. At this point, we can easily expand these integrals to any power of eccentricity. Because $J_p(qe) \sim (qe/2)^p/p!$ and, for $e \in (0,1)$, there is $\beta_e < e$, the series expansions of these integrals converge very rapidly. In practical calculations one usually determines the dynamical variables first and then evaluates the waveform. Hence, for a fixed eccentricity, the coefficients $\mathcal{L}$, the Bessel functions $J_p(qe)$, and even the generalized coefficients $\mathrm{J}^{(c)}_{pqa}$ themselves are repeatedly required. By caching these coefficients the computational cost can be reduced substantially. All of these integrals, together with the waveform routines discussed later, are packaged in the publicly available module `pyPNFourier`.

B. Results

1. *Solution of PN-Kepler equation*

Here we present the Fourier-series solution of the 4PN Kepler equation (5). We emphasize that the Kepler equation considered here does not include the contribution from the 4PN non-local effects.

First, we replace the orbital energy E and angular momentum J in the equation by v and e, and substitute the true anomaly ψ with χ_t. We then compute the Fourier series of $\chi - l$,

$$\chi - l \;=\; \sum_{p=1}^{\infty} X_p \sin pl. \tag{59}$$

The Fourier coefficients X_p have the structure

$$X_p = X_p^0 + v^4 X_p^2 + v^6 X_p^3 + v^8 X_p^4 + \mathcal{O}(c^{-9}), \tag{60}$$

$$X_p^0 = \frac{2}{p} J_p(ep) \tag{61}$$

$$\begin{aligned} X_p^2 = \frac{1}{\sqrt{1-e^2}} \Bigg[&(15-6\nu)\big(J_p(eq) + \mathrm{J}^{(1)}_{pp0}\big) - \frac{3}{2} e(5-2\nu)\big(2J_{p-1}(ep) + 2^{(+)}\mathrm{J}^{(1,1)}_{pp0} + 2p^{(-)}\mathrm{J}^{(1,1)}_{pp0} - ep^{(-)}\mathrm{J}^{(1,2)}_{pp0}\big) \\ &- \frac{1}{4} e\sqrt{1-e^2}(60 - 39\nu + \nu^2)^{(-)}\mathrm{J}^{(0,1)}_{pp0} \Bigg], \end{aligned} \tag{62}$$

$$\begin{aligned} X_p^3 = \frac{1}{(1-e^2)^{3/2}} \Bigg\{ &-\nu p(1-e^2)^{5/2}\left(\frac{13\nu^2}{48} - \frac{73\nu}{48} + \frac{23}{48}\right)\mathrm{J}^{(0)}_{pp1} + \Bigg[21\nu^2 + \left(\frac{41\pi^2}{32} - \frac{427}{3}\right)\nu + 60 \\ &- (1-e^2)(30 - 29\nu + 11\nu^2) + \nu p(1-e^2)^{3/2}\left(\frac{\nu^2}{12} + \frac{131\nu}{12} - \frac{505}{12}\right)\Bigg] J_p(ep) + \Bigg[10\nu^2 + \left(\frac{41\pi^2}{32} - \frac{340}{3}\right)\nu + 30 \\ &+ e^2(30 - 29\nu + 11\nu^2)\Bigg]\mathrm{J}^{(1)}_{pp0} + e\Bigg[e\left(\frac{13\nu^3}{24} - \frac{347\nu^2}{24} + \frac{86\nu}{3} - 30\right) + \sqrt{1-e^2}\Bigg(-\frac{13\nu^3}{24} - \frac{181\nu^2}{24} \\ &+ \left(\frac{12413}{210} - \frac{41\pi^2}{16}\right)\nu + 50\Bigg)\Bigg]^{(-)}\mathrm{J}^{(0,1)}_{pp1} + e\Bigg[5\nu^2 + \left(\frac{41\pi^2}{64} - \frac{170}{3}\right)\nu + 15 + e^2\left(\frac{11\nu^2}{2} - \frac{29\nu}{2} + 15\right)\Bigg]\big(ep^{(-)}\mathrm{J}^{(1,2)}_{pp0} \\ &- 2J_{p-1}(ep) - 2^{(+)}\mathrm{J}^{(1,1)}_{pp0} - 2p^{(-)}\mathrm{J}^{(1,1)}_{pp0}\big)\Bigg\} \end{aligned} \tag{63}$$

$$\begin{aligned} X_p^4 = \frac{1}{(1-e^2)^{5/2}} \Bigg\{ &\frac{9}{8} p(1-e^2)^{3/2}(5-2\nu)^2\big(4\mathrm{J}^{(2)}_{pp0} - 4e^{(+)}\mathrm{J}^{(2,1)}_{pp0} - 2ep^{(-)}\mathrm{J}^{(2,1)}_{pp0} + e^{2(-)}\mathrm{J}^{(2,2)}_{pp0}\big) \\ &+ \frac{3}{8}(1-e^2)^2(-300 + 315\nu - 83\nu^2 + 2\nu^3)\big(ep^{(-)}\mathrm{J}^{(1,1)}_{pp1} - \mathrm{J}^{(1)}_{pp1}\big) - \frac{3}{16}\nu(1-e^2)(75 - 35\nu + 2\nu^2)\big(e^2p^{2(+)}\mathrm{J}^{(1,2)}_{pp0} \\ &- 2(1-e^2)\mathrm{J}^{(1)}_{pp2}\big) + \Bigg[\nu p^2(1-e^2)^2(2-e^2)\left(\frac{3\nu^2}{8} - \frac{105\nu}{16} + \frac{225}{16}\right) - \frac{3}{2}\sqrt{1-e^2}\big(5(1-e^2) - 3\big)(5-2\nu)^2 - \frac{321\nu^3}{4} \\ &+ \left(\frac{8977}{8} - \frac{615\pi^2}{32}\right)\nu^2 + \left(\frac{47503\pi^2}{1024} - \frac{207253}{120}\right)\nu + \frac{2949}{8} + (1-e^2)\Bigg(\frac{171\nu^3}{2} + \frac{1}{96}\left(615\pi^2 - 64552\right)\nu^2 \end{aligned}$$

$$
\begin{aligned}
&+\Big(\frac{37567}{36}-\frac{53281\pi^2}{3072}\Big)\nu-\frac{2055}{8}\Big)+(1-e^2)^2\Big(-\frac{143\nu^3}{12}+\frac{403\nu^2}{24}-\frac{37\nu}{8}+15\Big)\Big]\mathrm{J}^{(1)}_{pp0}\\
&+\nu p(1-e^2)^{5/2}\Big(\Big(\frac{103e^2}{384}-\frac{107}{192}\Big)\nu^3+\Big(-\frac{35e^2}{64}-\frac{45}{32}\Big)\nu^2+\Big(\frac{85e^2}{128}-\frac{41\pi^2}{128}-\frac{92303}{4032}\Big)\nu+\frac{349e^2}{384}-\frac{903\pi^2}{1024}\\
&-\frac{7111577}{201600}\Big)\mathrm{J}^{(0)}_{pp1}+\nu p(1-e^2)^{7/2}\Big(\frac{5\nu^3}{64}-\frac{187\nu^2}{32}+\frac{20269\nu}{576}-\frac{1447}{144}\Big)\mathrm{J}^{(0)}_{pp2}+\nu p(1-e^2)^{9/2}\Big(\frac{25\nu^3}{256}+\frac{27\nu^2}{128}-\frac{1639\nu}{256}\\
&-\frac{31}{256}\Big)\mathrm{J}^{(0)}_{pp3}+e\Big(\frac{321\nu^3}{4}+\frac{1}{32}\Big(615\pi^2-35908\Big)\nu^2+\Big(\frac{207253}{120}-\frac{47503\pi^2}{1024}\Big)\nu-\frac{2949}{8}+e^2\Big(-\frac{171\nu^3}{2}\\
&-\frac{1}{96}\Big(615\pi^2-64552\Big)\nu^2+\Big(\frac{53281\pi^2}{3072}-\frac{37567}{36}\Big)\nu+\frac{2055}{8}\Big)+e^4\Big(\frac{143\nu^3}{12}-\frac{403\nu^2}{24}+\frac{37\nu}{8}-15\Big)\\
&+\frac{3}{2}\sqrt{1-e^2}\big(2(1-e^2)-3\big)(5-2\nu)^2-\frac{1}{32}\nu^2p^2(1-e^2)\Big)J_{p-1}(ep)+\Big[p(1-e^2)^{3/2}\Big(-\frac{45\nu^3}{4}+\Big(\frac{135\pi^2}{8}-\frac{274069}{2520}\Big)\nu^2\\
&+\Big(\frac{1730437}{4200}-\frac{34135\pi^2}{3072}\Big)\nu-\frac{1695}{8}+\nu\sqrt{1-e^2}\Big(-\frac{9\nu^2}{4}+\frac{315\nu}{8}-\frac{675}{8}\Big)+\nu(1-e^2)\Big(\frac{5\nu^3}{192}+\frac{639\nu^2}{32}\\
&-\frac{5699\nu}{192}-\frac{1135}{96}\Big)\Big)+\frac{1}{32}\nu^2p^2(1-e^2)^{5/2}(15-\nu)^2+\frac{3}{2}\sqrt{1-e^2}(5-2\nu)^2\big(1+2e^2\big)-\frac{321\nu^3}{4}+\Big(\frac{8977}{8}-\frac{615\pi^2}{32}\Big)\nu^2\\
&+\Big(\frac{47503\pi^2}{1024}-\frac{207253}{120}\Big)\nu+\frac{2949}{8}+(1-e^2)\Big(\frac{171\nu^3}{2}+\Big(\frac{205\pi^2}{32}-\frac{8069}{12}\Big)\nu^2+\Big(\frac{37567}{36}-\frac{53281\pi^2}{3072}\Big)\nu-\frac{2055}{8}\Big)\\
&+(1-e^2)^2\Big(-\frac{143\nu^3}{12}+\frac{403\nu^2}{24}-\frac{37\nu}{8}+15\Big)\Big]J_p(ep)+e\Big[-\frac{3}{2}\sqrt{1-e^2}(1+2e^2)(5-2\nu)^2+\frac{20\nu^3}{3}\\
&+\Big(\frac{205\pi^2}{16}-\frac{933}{2}\Big)\nu^2+\Big(\frac{123877}{180}-\frac{22307\pi^2}{768}\Big)\nu-\frac{507}{4}+e^2\Big(\frac{185\nu^3}{3}+\Big(\frac{205\pi^2}{32}-\frac{3833}{6}\Big)\nu^2+\Big(\frac{18617}{18}-\frac{53281\pi^2}{3072}\Big)\nu\\
&-\frac{1815}{8}\Big)+e^4\Big(\frac{143\nu^3}{12}-\frac{403\nu^2}{24}+\frac{37\nu}{8}-15\Big)\Big]{}^{(+)}\mathrm{J}^{(1,1)}_{pp0}+ep\Big[\frac{3}{2}\sqrt{1-e^2}(2-5e^2)(5-2\nu)^2+\frac{49\nu^3}{6}+\Big(\frac{205\pi^2}{16}-\frac{1971}{4}\Big)\nu^2\\
&+\Big(\frac{67001}{90}-\frac{22307\pi^2}{768}\Big)\nu-\frac{507}{4}+e^2\Big(\frac{176\nu^3}{3}+\Big(\frac{205\pi^2}{32}-\frac{1759}{3}\Big)\nu^2+\Big(\frac{8296}{9}-\frac{53281\pi^2}{3072}\Big)\nu-\frac{1815}{8}\Big)\\
&+e^4\Big(\frac{161\nu^3}{12}-\frac{1033\nu^2}{24}+\frac{487\nu}{8}-15\Big)\Big]{}^{(-)}\mathrm{J}^{(1,1)}_{pp0}+e\Big[\sqrt{1-e^2}\Big[\frac{141\nu^3}{2}+\Big(-\frac{619691}{1260}-\frac{335\pi^2}{16}\Big)\nu^2+\Big(\frac{2584979}{6300}+\frac{99\pi^2}{64}\Big)\nu\\
&+107+(1-e^2)\Big(-\frac{1123\nu^3}{12}+\Big(\frac{69581}{120}-\frac{697\pi^2}{64}\Big)\nu^2+\Big(\frac{67951\pi^2}{3072}-\frac{10111811}{12600}\Big)\nu+\frac{135}{8}\Big)+(1-e^2)^2\Big(-\frac{283\nu^4}{576}\\
&+\frac{1231\nu^3}{96}-\frac{2141\nu^2}{192}+\frac{241\nu}{192}-15\Big)\Big]+(1-e^2)^2\Big(-\frac{\nu^3}{2}+\frac{83\nu^2}{4}-\frac{315\nu}{4}+75\Big)-\frac{1}{64}\nu^2p^2(15-\nu)^2\Big]{}^{(-)}\mathrm{J}^{(0,1)}_{pp1}\\
&+e^2p\Big[\frac{3}{4}\sqrt{1-e^2}(1+2e^2)(5-2\nu)^2+-\frac{321\nu^3}{8}+\Big(\frac{8977}{16}-\frac{615\pi^2}{64}\Big)\nu^2+\Big(\frac{47503\pi^2}{2048}-\frac{207253}{240}\Big)\nu+\frac{2949}{16}\\
&+(1-e^2)\Big(\frac{171\nu^3}{4}+\Big(\frac{205\pi^2}{64}-\frac{8069}{24}\Big)\nu^2+\Big(\frac{37567}{72}-\frac{53281\pi^2}{6144}\Big)\nu-\frac{2055}{16}\Big)+(1-e^2)^2\Big(-\frac{143\nu^3}{24}+\frac{403\nu^2}{48}\\
&-\frac{37\nu}{16}+\frac{15}{2}\Big)\Big]{}^{(-)}\mathrm{J}^{(1,2)}_{pp0}\Big\},
\end{aligned}\tag{64}
$$

where we introduce shorthands

$$
{}^{(\pm)}\mathrm{J}^{(b,c)}_{pqa}:=\frac{1}{2}\Big(\mathrm{J}^{(b)}_{(p+c)qa}\pm\mathrm{J}^{(b)}_{(p-c)qa}\Big),\tag{65}
$$

(66)

2. Multipole moments

There are two sets of radiative-type multipole moments U_L, V_L [73], where $L = i_1...i_l$ denotes the (STF) multi-indices. These radiative-type moments is determined by six source-type moments $(I_L, J_L, W_L, X_L, Y_L, Z_L)$ or two kinds of canonical source-type multipole moments M_L, S_L,

$$U_L(t_r) = M_L^{(\ell)}(t_r) + \frac{2M_{\text{ADM}}}{c^3}\int_0^\infty \mathrm{d}\tau M_L^{(\ell+2)}(t_r-\tau)\Big[\ln\Big(\frac{\tau}{2r_0}\Big)+\kappa_\ell\Big] + \mathcal{O}\big(c^{-5}\big), \tag{67}$$

$$V_L(t_r) = S_L^{(\ell)}(t_r) + \frac{2M_{\text{ADM}}}{c^3}\int_0^\infty \mathrm{d}\tau S_L^{(\ell+2)}(t_r-\tau)\Big[\ln\Big(\frac{\tau}{2r_0}\Big)+\pi_\ell\Big] + \mathcal{O}\big(c^{-5}\big), \tag{68}$$

where t_r denotes retarded-time and M_{ADM} is ADM mass. At same PN-level, the number of the indices of V is 1 less than U. At present, we have a clear understanding of the form of 3PN in the MH frame [90, 91], and recently the 4PN results were published [92]. In this work, we are concerned with the form of 3PN in the MH frame [93]. Following [90], the structure of the Fourier decomposition of M_L, S_L reads

$$M_L = \sum_{m=-\ell}^{\ell}\sum_{p=-\infty}^{\infty} \underset{(p,m)}{\mathrm{M}_L}\, \mathrm{e}^{\mathrm{i}(m\lambda+pl)}, \tag{69}$$

$$S_L = \sum_{m=-\ell}^{\ell}\sum_{p=-\infty}^{\infty} \underset{(p,m)}{\mathrm{S}_L}\, \mathrm{e}^{\mathrm{i}(m\lambda+pl)}. \tag{70}$$

To expand these moments, we use polar coordinates $(r, \dot{r}, \phi, \dot{\phi})$, then

$$(x, y, z) = r(\cos\phi, \sin\phi, 0), \tag{71}$$

$$(v_x, v_y, v_z) = (\dot{r}\cos\phi - r\dot{\phi}\sin\phi, \dot{r}\sin\phi + r\dot{\phi}\cos\phi, 0). \tag{72}$$

In this coordinates, the STF matrices can be represented by $(r, \dot{r}, \dot{\phi})$. Substituting the results of the quasi-Keplerian expansion and then performing Fourier integration, we obtain the Fourier modes of these moments. Here we show the 2PN results of M_{xx} as an example, the results of higher PN order and the other moments are showed in supplementary material,

$$\underset{(p,2)}{\mathrm{M}_{xx}} = \frac{\nu}{v^4}\Big(\underset{(p,2)}{\mathrm{M}^N_{xx}} + v^2\underset{(p,2)}{\mathrm{M}^{\text{1PN}}_{xx}} + v^4\underset{(p,2)}{\mathrm{M}^{\text{2PN}}_{xx}} + v^5\underset{(p,2)}{\mathrm{M}^{\text{2.5PN}}_{xx}} + v^6\underset{(p,2)}{\mathrm{M}^{\text{3PN}}_{xx}} + \mathcal{O}\big(c^{-7}\big)\Big), \tag{73}$$

$$\underset{(p-2,2)}{\mathrm{M}^N_{xx}} = \frac{1}{e^2p^2}\Bigg[e\sqrt{1-e^2}\big(-1+\sqrt{1-e^2}p\big)J_{p-1}\big(ep\big) + \frac{1}{2}\big(-1+\sqrt{1-e^2}\big)\big(-1+\sqrt{1-e^2}-2(1-e^2)p\big)J_p\big(ep\big)\Bigg], \tag{74}$$

$$\begin{aligned}\underset{(p-2,2)}{\mathrm{M}^{\text{1PN}}_{xx}} = {} & \frac{1}{e^2(1-e^2)p^3}\Bigg\{\frac{3}{8}e^2p^3\Big[5e(2+e^2)^{(+)}\mathrm{J}^{(1,1)}_{pp0} - 2(2+e^2)^{(+)}\mathrm{J}^{(1,2)}_{pp0} + e(2-e^2)^{(+)}\mathrm{J}^{(1,3)}_{pp0}\Big] + \frac{3}{4}e^2\sqrt{1-e^2}p^3\Big[2(1+e^2)^{(-)}\mathrm{J}^{(1,2)}_{pp0} \\ & - e^{(-)}\mathrm{J}^{(1,3)}_{pp0} - 5e^{(-)}\mathrm{J}^{(1,1)}_{pp0}\Big] - \frac{15}{4}e^4p^3\mathrm{J}^{(1)}_{pp0} + e\Bigg[\sqrt{1-e^2}\Bigg[18 - p\nu - p^2(1-e^2)\Bigg(\frac{23}{42}+\frac{4\nu}{21}\Bigg) + p^3(1-e^2)^2\Bigg(\frac{1}{21}-\frac{\nu}{7}\Bigg)\Bigg] - \frac{15}{2}p \\ & + (1-e^2)\Bigg(\frac{27}{14}\nu p^2 + \frac{3}{14}(-10p-91)p\Bigg) - (1-e^2)^2p^2\Bigg(\frac{23}{42}+\frac{4\nu}{21}\Bigg)\Bigg]J_{p+1}\big(ep\big) + \big(1-\sqrt{1-e^2}\big)\Bigg[9+\frac{11}{2}p \\ & + (1-e^2)\Bigg(\frac{1}{84}\nu p(-162p-67) + \frac{1}{84}p(180p+1539)\Bigg) + (1-e^2)^2p^2\Bigg(\frac{11}{21}+\frac{11\nu}{42}\Bigg) + \sqrt{1-e^2}\Bigg[\nu p - \frac{13p}{2} - 9 \\ & + (1-e^2)\Bigg(\frac{1}{84}\nu p(6p-17) + \frac{1}{84}p(57-758p)\Bigg) + (1-e^2)^2p^3\Bigg(-\frac{1}{21}+\frac{\nu}{7}\Bigg)\Bigg]\Bigg]J_p\big(ep\big)\Bigg\},\end{aligned} \tag{75}$$

$$\begin{aligned}\underset{(p-2,2)}{\mathrm{M}^{\text{2PN}}_{xx}} = {} & \frac{1}{e^2p^4(1-e^2)^2}\Bigg\{e^4p^4\Bigg[(1-e^2)\Bigg(\frac{249}{16}-\frac{17\nu}{4}\Bigg) + \Bigg(1-e^2\Bigg)^{3/2}\Bigg(\frac{75p}{16}-\frac{15\nu p}{8}\Bigg) - \frac{45\sqrt{1-e^2}}{4} + \frac{135\nu}{8} - \frac{765}{16}\Bigg]\mathrm{J}^{(1)}_{pp0} \\ & + \frac{45e^4p^4}{4}\mathrm{J}^{(2)}_{pp0} + (1-e^2)^4p^4\Bigg(\frac{613\nu^2}{3024} - \frac{7195\nu}{3024} + \frac{4513}{1512}\Bigg)\mathrm{J}^{(0)}_{pp1} + (1-e^2)^5p^4\Bigg(-\frac{613\nu^2}{3024} + \frac{2011\nu}{3024} + \frac{131}{1512}\Bigg)\mathrm{J}^{(0)}_{pp2}\end{aligned}$$

$$+e\Bigg[\bigg(\frac{\nu^2}{16}-\frac{15\nu}{16}\bigg)p^5(1-e^2)^4+\bigg(\frac{9\nu}{14}-\frac{97}{28}\bigg)p^4(1-e^2)^3+p^3\Bigg(\bigg(-\frac{53\nu^2}{168}+\frac{655\nu}{504}+\frac{2}{7}\bigg)(1-e^2)^3$$

$$+\bigg(\frac{197\nu^2}{126}+\frac{344\nu}{63}+\frac{7375}{504}\bigg)(1-e^2)^2+\bigg(-\frac{149\nu}{14}-\frac{207}{14}\bigg)(1-e^2)\Bigg)+p^2\bigg(\frac{135\nu}{4}+\bigg(\frac{4579}{56}-\frac{531\nu}{14}\bigg)(1-e^2)^2$$

$$+\bigg(\frac{515\nu}{28}-\frac{180}{7}\bigg)(1-e^2)-\frac{765}{8}\bigg)+p\big(252(1-e^2)+144\big)+\sqrt{1-e^2}\Bigg[p^4\Bigg(\bigg(\frac{73\nu^2}{378}-\frac{19\nu}{54}+\frac{149}{1512}\bigg)(1-e^2)^3$$

$$+\bigg(\frac{32\nu^2}{189}+\frac{437\nu}{378}+\frac{8989}{756}\bigg)(1-e^2)^2\Bigg)+p^3\Bigg(\bigg(\frac{397\nu}{28}-\frac{1891}{56}\bigg)(1-e^2)^2+\bigg(\frac{347}{8}-\frac{63\nu}{4}\bigg)(1-e^2)\Bigg)+p^2\bigg(\frac{\nu^2}{2}+\frac{17\nu}{2}$$

$$+\bigg(-\frac{5\nu^2}{24}-\frac{15\nu}{56}+\frac{85}{168}\bigg)(1-e^2)^2+\bigg(-\frac{37\nu^2}{21}-\frac{19\nu}{6}-\frac{2955}{28}\bigg)(1-e^2)-\frac{361}{4}\bigg)+p\bigg(-63\nu$$

$$+\bigg(\frac{348\nu}{7}-\frac{1737}{14}\bigg)(1-e^2)+\frac{315}{2}\bigg)-216\Bigg]\Bigg]J_{p-1}(ep)+\Bigg[\bigg(\frac{15\nu}{16}-\frac{\nu^2}{16}\bigg)p^5(1-e^2)^4+p^4\Bigg(\bigg(\frac{31\nu^2}{252}-\frac{41\nu}{84}$$

$$+\frac{143}{1008}\bigg)(1-e^2)^4+\bigg(\frac{181\nu^2}{756}+\frac{1787\nu}{756}+\frac{37013}{3024}\bigg)(1-e^2)^3\Bigg)+p^3\Bigg(\bigg(\frac{53\nu^2}{168}+\frac{6653\nu}{504}-\frac{501}{14}\bigg)(1-e^2)^3$$

$$+\bigg(-\frac{197\nu^2}{126}-\frac{2713\nu}{126}+\frac{15359}{504}\bigg)(1-e^2)^2+\bigg(\frac{149\nu}{14}+\frac{207}{14}\bigg)(1-e^2)\Bigg)+p^2\bigg(-\frac{99\nu}{4}+\bigg(\frac{3\nu^2}{112}+\frac{37\nu}{48}-\frac{155}{336}\bigg)(1-e^2)^3$$

$$+\bigg(-\frac{503\nu^2}{336}+\frac{4385\nu}{112}-\frac{9419}{48}\bigg)(1-e^2)^2+\bigg(-\frac{681\nu}{28}-\frac{253}{7}\bigg)(1-e^2)+\frac{617}{8}\bigg)+p\bigg(-\frac{81\nu}{2}$$

$$+\bigg(\frac{111\nu}{7}-\frac{729}{28}\bigg)(1-e^2)^2+\bigg(\frac{159\nu}{14}-\frac{2151}{7}\bigg)(1-e^2)-\frac{117}{4}\bigg)-108(1-e^2)-108+\sqrt{1-e^2}\Bigg[\bigg(-\frac{53\nu^2}{378}-\frac{103\nu}{378}$$

$$+\frac{131}{1512}\bigg)p^5(1-e^2)^4+p^4\Bigg(\bigg(-\frac{73\nu^2}{378}+\frac{188\nu}{189}-\frac{5387}{1512}\bigg)(1-e^2)^3+\bigg(-\frac{32\nu^2}{189}-\frac{437\nu}{378}-\frac{8989}{756}\bigg)(1-e^2)^2\Bigg)$$

$$+p^3\Bigg(\bigg(\frac{149\nu^2}{504}-\frac{317\nu}{168}+\frac{295}{504}\bigg)(1-e^2)^3+\bigg(\frac{19\nu^2}{42}-\frac{185\nu}{63}+\frac{443}{8}\bigg)(1-e^2)^2+\bigg(\frac{\nu^2}{2}+\frac{211\nu}{84}-\frac{10993}{168}\bigg)(1-e^2)\Bigg)$$

$$+p^2\bigg(-\frac{\nu^2}{2}+\frac{67\nu}{2}+\bigg(\frac{5\nu^2}{24}-\frac{239\nu}{8}+\frac{1799}{24}\bigg)(1-e^2)^2+\bigg(\frac{37\nu^2}{21}+\frac{116\nu}{21}+\frac{191}{2}\bigg)(1-e^2)-\frac{59}{4}\bigg)+p\bigg(63\nu$$

$$+\bigg(\frac{4005}{14}-\frac{348\nu}{7}\bigg)(1-e^2)+\frac{153}{2}\bigg)+216\Bigg]\Bigg]J_p(ep)+e^3\Bigg[p^4\bigg(-\frac{405\nu}{16}+\bigg(\frac{1055}{224}-\frac{65\nu}{56}\bigg)(1-e^2)^2$$

$$+\bigg(\frac{1983\nu}{112}-\frac{1581}{28}\bigg)(1-e^2)+\frac{2295}{32}\bigg)+\sqrt{1-e^2}\Bigg[p^5\Bigg(\bigg(\frac{75}{32}-\frac{15\nu}{16}\bigg)(1-e^2)^2+\bigg(\frac{45\nu}{16}-\frac{225}{32}\bigg)(1-e^2)\Bigg)$$

$$+p^4\bigg(9-\frac{9(1-e^2)}{2}\bigg)\Bigg]\Bigg]{}^{(+)}\mathrm{J}^{(1,1)}_{pp0}-\frac{45}{8}e^3p^4(1+2e^2){}^{(+)}\mathrm{J}^{(2,1)}_{pp0}+e^2\Bigg[p^4\bigg(\frac{81\nu}{8}+\bigg(\frac{55\nu}{28}-\frac{883}{112}\bigg)(1-e^2)^2$$

$$+\bigg(\frac{471}{14}-\frac{591\nu}{56}\bigg)(1-e^2)-\frac{459}{16}\bigg)+\sqrt{1-e^2}\Bigg[p^5\Bigg(\bigg(\frac{3\nu}{8}-\frac{15}{16}\bigg)(1-e^2)^2+\bigg(\frac{45}{16}-\frac{9\nu}{8}\bigg)(1-e^2)\Bigg)$$

$$+p^4\big(9-9(1-e^2)\big)\Bigg]\Bigg]{}^{(+)}\mathrm{J}^{(1,2)}_{pp0}+\frac{9}{4}e^2p^4(1+2e^2){}^{(+)}\mathrm{J}^{(2,2)}_{pp0}+e^2\Bigg[p^4\bigg(-\frac{27e\nu}{16}+(1-e^2)^2\bigg(\frac{37e\nu}{56}-\frac{243e}{224}\bigg)$$

$$+(1-e^2)\bigg(\frac{53e\nu}{112}-\frac{129e}{56}\bigg)+\frac{153e}{32}\bigg)+\sqrt{1-e^2}\Bigg[p^5\bigg((1-e^2)^2\bigg(\frac{3e\nu}{16}-\frac{15e}{32}\bigg)+(1-e^2)\bigg(\frac{3e\nu}{16}-\frac{15e}{32}\bigg)\bigg)$$

$$+p^4\bigg(\frac{9e(1-e^2)}{2}-9e\bigg)\Bigg]\Bigg]{}^{(+)}\mathrm{J}^{(1,3)}_{pp0}+\frac{9}{8}e^3p^4(-2+e^2){}^{(+)}\mathrm{J}^{(2,3)}_{pp0}+\frac{9}{4}e^4p^4\sqrt{1-e^2}{}^{(+)}\mathrm{J}^{(1,4)}_{pp0}+e^3\Bigg[\bigg(\frac{75}{16}-\frac{15\nu}{8}\bigg)p^5(1-e^2)^2$$

$$+p^4\bigg(\frac{63}{4}-\frac{81(1-e^2)}{4}\bigg)+\sqrt{1-e^2}p^4\bigg[\frac{105\nu}{8}+\bigg(\frac{1439}{112}-\frac{61\nu}{14}\bigg)(1-e^2)-\frac{525}{16}\bigg]\Bigg]{}^{(-)}\mathrm{J}^{(1,1)}_{pp0}+\frac{45}{4}e^3p^4\sqrt{1-e^2}{}^{(-)}\mathrm{J}^{(2,1)}_{pp0}$$

$$+ep^4(1-e^2)^{7/2}\bigg(-\frac{43}{14}+\frac{12}{7}\nu\bigg){}^{(-)}\mathrm{J}^{(0,1)}_{pp1}+e^2\Bigg[p^5\Bigg(\bigg(\frac{15}{8}-\frac{3\nu}{4}\bigg)(1-e^2)^3+\bigg(\frac{3\nu}{2}-\frac{15}{4}\bigg)(1-e^2)^2\Bigg)$$

$$+p^4\bigg(-\frac{27(1-e^2)^2}{4}+\frac{45(1-e^2)}{2}-\frac{63}{4}\bigg)+\sqrt{1-e^2}p^4\bigg[-\frac{21\nu}{2}+\bigg(\frac{223}{56}-\frac{11\nu}{7}\bigg)(1-e^2)^2$$
$$+\bigg(\frac{295\nu}{28}-\frac{1529}{56}\bigg)(1-e^2)+\frac{105}{4}\bigg]\bigg]{}^{(-)}\mathrm{J}^{(1,2)}_{pp0}-\frac{9}{2}e^2p^4\sqrt{1-e^2}(1+e^2){}^{(-)}\mathrm{J}^{(2,2)}_{pp0}+e^3p^4\bigg[\bigg(\frac{15}{16}-\frac{3\nu}{8}\bigg)p(1-e^2)^2-\frac{9(1-e^2)}{4}$$
$$+\frac{27}{4}+\sqrt{1-e^2}\bigg[\frac{21\nu}{8}+\bigg(\frac{579}{112}-\frac{29\nu}{14}\bigg)(1-e^2)-\frac{105}{16}\bigg]\bigg]{}^{(-)}\mathrm{J}^{(1,3)}_{pp0}+\frac{9}{4}e^3p^4\sqrt{1-e^2}{}^{(-)}\mathrm{J}^{(2,3)}_{pp0}+\frac{9}{8}e^4p^4(-2+e^2){}^{(-)}\mathrm{J}^{(1,4)}_{pp0}\bigg\},\tag{76}$$

where the 1PN results are consistent with [94].

3. *Gravitational waveform*

The GWs emitted to null infinity can be expressed in transverse-traceless frame h_{ij}^{TT} constituted by two polarizations $h_+, h_\times$. The perturbation matrix h_{ij}^{TT} can be uniquily decomposed in to radiative-type multipole moments [71]

$$h_{ij}^{\mathrm{TT}}=\frac{4}{c^2R}P_{ijab}^{\mathrm{TT}}(\boldsymbol{N})\sum_{l=2}^{\infty}\frac{1}{c^l l!}\bigg[N_{L-2}U_{ab(L-2)}-\frac{2\ell}{c(\ell+1)}N_{c(L-2)}\epsilon_{cd(a}V_{b)d(L-2)}\bigg]+\mathcal{O}\big(R^{-2}\big),\tag{77}$$

where $\boldsymbol{N}=(\sin\theta\cos\phi,\sin\theta\sin\phi,\cos\theta)$ is the direction from the source to the observer, R denotes the (luminosity) distance of the source, and P_{ijab}^{TT} is transverse-traceless projector. The GW polarization can be decomposed by spin-weighted -2 spherical harmonics [93]

$$h_+-\mathrm{i}h_\times=\sum_{l=2}^{\infty}\sum_{m=-\ell}^{\ell}h_{\ell m}[{}_{-2}Y_{\ell m}](\theta,\phi).\tag{78}$$

The spherical harmonic modes are given by

$$h_{\ell m}=-\frac{1}{\sqrt{2}Rc^{\ell+2}}\Big(U_{\ell m}-\frac{\mathrm{i}}{c}V_{\ell m}\Big),\tag{79}$$

where the spherical modes of the radiative moments U_{lm}, V_{lm} are

$$U_{\ell m}=\frac{4}{\ell!}\sqrt{\frac{(\ell+1)(\ell+2)}{2\ell(\ell-1)}}\alpha_L^{\ell m}U_L,\tag{80}$$
$$V_{\ell m}=-\frac{8}{\ell!}\sqrt{\frac{\ell(\ell+2)}{2(\ell+1)(\ell-2)}}\alpha_L^{\ell m}V_L.\tag{81}$$

The coefficient $\alpha_L^{\ell m}$ denotes the connection between STF tensor $N^{\langle L\rangle}$ and spherical harmonics Y_{lm} [95],

$$N^{\langle L\rangle}=\sum_{m=-\ell}^{\ell}\alpha^L_{\ell m}(\boldsymbol{N})Y_{\ell m}(\boldsymbol{N}),\tag{82}$$
$$Y_{\ell m}(\boldsymbol{N})=\frac{(2\ell+1)!!}{4\pi\ell!}\alpha^{L*}_{\ell m}(\boldsymbol{N})N^{\langle L\rangle},\tag{83}$$
$$\alpha_L^{\ell m}:=\int\mathrm{d}\boldsymbol{N}N^{\langle L\rangle}Y^*_{\ell m}(\boldsymbol{N}).\tag{84}$$

The GW waveform includes instantaneous part, tail part, and memory part, which correspond to the three components of the radiation multipole moment respectively. For higher PN orders exceeding 3PN, there will also be a tail-memory interaction part. Currently, we only consider the instantaneous part and the tail part within 3PN. When calculating the tail part, one would encounter integrals involving the power of logarithm. To evaluate such integral, one can use

$$\frac{\mathrm{d}^s\Gamma(z)}{\mathrm{d}z^s}\bigg|_{z=1}=\int_0^\infty\mathrm{d}\tau e^{-\tau}\ln^s\tau.\tag{85}$$

Therefore,

$$
\begin{aligned}
\int_0^\infty \mathrm{e}^{-\mathrm{i}y\tau}\ln^s\tau\mathrm{d}\tau &= \frac{\partial^s}{\partial z^s}\int_0^\infty t^{z-1}\mathrm{e}^{-(\varepsilon+\mathrm{i}y)\tau}\mathrm{d}\tau\Big|_{z=1,\varepsilon=0} = \frac{\partial^s}{\partial z^s}\Big[(\varepsilon+\mathrm{i}y)^{-z}\Gamma(z)\Big]\Big|_{z=1,\varepsilon=0} \\
&= \frac{1}{\mathrm{i}y}\sum_{m=0}^{s}(-1)^m\binom{s}{m}\bar{\boldsymbol{\gamma}}_{s-m}\Big(\ln|y|+\mathrm{sgn}(y)\frac{\pi}{2}\Big)^m, \qquad (86)
\end{aligned}
$$

where $\bar{\boldsymbol{\gamma}}_s := \frac{\mathrm{d}^s}{\mathrm{d}z^s}\Gamma(z)\big|_{z=1}$. This formula can recover [96]. Substituting the Fourier expansion of M_L, S_L and integrating, one could express the Fourier modes in terms of $\mathrm{J}^{(n)}_{pqa}$. Here we show 2PN results of h_{22} for example, the results of higher PN order and other spherical modes can be found in supplementary material,

$$
h_{22} = \sqrt{\frac{\pi}{5}}\frac{4\nu v^2}{c^4 R}\mathrm{e}^{-\mathrm{i}2\lambda}\sum_{p=-\infty}^{\infty}\tilde{H}_{2(-2)p}\mathrm{e}^{\mathrm{i}pl}, \qquad (87)
$$

$$
\begin{aligned}
\tilde{H}_{2(-2)p} &= \tilde{H}^N_{2(-2)p} + \frac{1}{c^2}v^2\tilde{H}^{\mathrm{1PN}}_{2(-2)p} + \frac{1}{c^3}v^3\tilde{H}^{\mathrm{tail,1.5PN}}_{2(-2)p} + \frac{1}{c^4}v^4\tilde{H}^{\mathrm{2PN}}_{2(-2)p} + \frac{1}{c^5}v^5\Big(\tilde{H}^{\mathrm{2.5PN}}_{2(-2)p} + \tilde{H}^{\mathrm{tail,2.5PN}}_{2(-2)p}\Big) \\
&\quad + \frac{1}{c^6}v^6\Big(\tilde{H}^{\mathrm{3PN}}_{2(-2)p} + \tilde{H}^{\mathrm{tail,3PN}}_{2(-2)p}\Big) + \mathcal{O}(c^{-7}), \qquad (88)
\end{aligned}
$$

$$
\begin{aligned}
\tilde{H}^N_{2(-2)(p+2)} &= \frac{1}{e^2}\Bigg[(-2+2e^2)\mathrm{J}^{(0)}_{pp1} + (2-4e^2+2e^4)\mathrm{J}^{(0)}_{pp2} + 2e\sqrt{1-e^2}J_{p-1}(ep) \\
&\quad + \Big[e^2-2-2\sqrt{1-e^2}(1+p-e^2p)\Big]J_p(ep)\Bigg] \qquad (89)
\end{aligned}
$$

$$
\begin{aligned}
\tilde{H}^{\mathrm{1PN}}_{2(-2)(p+2)} &= \frac{1}{e^2p(1-e^2)}\Bigg\{-12p^2(1-e^2)^{3/2}\mathrm{J}^{(1)}_{pp0} - 12p(1-e^2)\mathrm{J}^{(1)}_{pp1} + p(1-e^2)\Bigg[e^2\Big(-\frac{8\nu}{21}-\frac{23}{21}\Big) - \frac{73\nu}{21} + \frac{113}{21} \\
&\quad + \sqrt{1-e^2}\Bigg[p\Bigg(e^2\Big(\frac{2\nu}{7}+\frac{124}{21}\Big) - \frac{2\nu}{7} - \frac{124}{21}\Bigg) - 12\Bigg]\Bigg]\mathrm{J}^{(0)}_{pp1} + p(1-e^2)\Bigg[e^4\Big(-\frac{20\nu}{21}-\frac{19}{21}\Big) + e^2\Big(\frac{884}{21}-\frac{41\nu}{21}\Big) \\
&\quad + \frac{61\nu}{21} - \frac{865}{21} + \sqrt{1-e^2}\Bigg[-12e^2 + p\Bigg(e^4\Big(\frac{2\nu}{7}-\frac{2}{21}\Big) + e^2\Big(\frac{4}{21}-\frac{4\nu}{7}\Big) + \frac{2\nu}{7} - \frac{2}{21}\Bigg) + 12\Bigg]\Bigg]\mathrm{J}^{(0)}_{pp2} + 12p(1-e^2)^2\mathrm{J}^{(1)}_{pp2} \\
&\quad + p(1-e^2)\Bigg[e^4\Big(\frac{10\nu}{7}+\frac{242}{21}\Big) + e^2\Big(-\frac{20\nu}{7}-\frac{484}{21}\Big) + \frac{10\nu}{7} + \frac{242}{21}\Bigg]\mathrm{J}^{(0)}_{pp3} + p(1-e^2)\Bigg[e^6\Big(\frac{6\nu}{7}-\frac{2}{7}\Big) + e^4\Big(\frac{6}{7}-\frac{18\nu}{7}\Big) \\
&\quad + e^2\Big(\frac{18\nu}{7}-\frac{6}{7}\Big) - \frac{6\nu}{7} + \frac{2}{7}\Bigg]\mathrm{J}^{(0)}_{pp4} + e\Bigg[p(12-6e^2) + \sqrt{1-e^2}\Bigg[p\Bigg(e^2\Big(\frac{37}{7}-\frac{25\nu}{21}\Big) + \frac{67\nu}{21} - \frac{121}{7}\Bigg) + 12\Bigg]\Bigg]J_{p-1}(ep) \\
&\quad + \Bigg[6e^2 + \Big(-12e^4+24e^2-12\Big)p^2 + p\Bigg(e^4\Big(\frac{17\nu}{42}-\frac{19}{14}\Big) + e^2\Big(\frac{39\nu}{14}-\frac{279}{14}\Big) - \frac{67\nu}{21} + \frac{121}{7}\Bigg) - 12 \\
&\quad + \sqrt{1-e^2}\Bigg[p\Bigg(e^2\Big(\frac{25\nu}{21}-\frac{37}{7}\Big) - \frac{67\nu}{21} + \frac{121}{7}\Bigg) + p^2\Bigg(e^4\Big(\frac{11\nu}{21}+\frac{22}{21}\Big) + e^2\Big(\frac{62\nu}{21}-\frac{129}{7}\Big) - \frac{73\nu}{21} + \frac{365}{21}\Bigg) - 12\Bigg]\Bigg]J_p(ep) \\
&\quad + ep(-12+6e^2)^{(+)}\mathrm{J}^{(1,1)}_{pp0} - 12ep\sqrt{1-e^2}{}^{(-)}\mathrm{J}^{(1,1)}_{pp0} - 6ep\Big[2(1-e^2)+\sqrt{1-e^2}(2-e^2)\Big]{}^{(-)}\mathrm{J}^{(0,1)}_{pp1}\Bigg\} \qquad (90)
\end{aligned}
$$

$$
\begin{aligned}
\tilde{H}^{\mathrm{tail,1.5PN}}_{2(-2)(p+2)} &= \frac{\mathrm{i}}{e^2p}\Bigg(3\ln\Big(\frac{x}{x_0'}\Big) + 2\ln\Big(\frac{\mathrm{i}p}{2}\Big)\Bigg)\Bigg[p\sqrt{1-e^2}\mathrm{J}^{(0)}_{pp1} + \Big[2-e^2+p(1-e^2)^{3/2}\Big]\mathrm{J}^{(0)}_{pp2} + \Big[1-\frac{7}{2}e^2 \\
&\quad - p(1-e^2)^{3/2}\Big]\mathrm{J}^{(0)}_{pp3} + \Big[-\frac{21e^4}{2}+\frac{67e^2}{2}-23+3p(1-e^2)^{5/2}\Big]\mathrm{J}^{(0)}_{pp4} + 35(1-e^2)^2\mathrm{J}^{(0)}_{pp5} + 15(1-e^2)^3\mathrm{J}^{(0)}_{pp6}\Bigg] \qquad (91)
\end{aligned}
$$

$$
\tilde{H}^{\mathrm{2PN}}_{2(-2)(p+2)} = \frac{1}{e^2p^2(1-e^2)^2}\Bigg\{p^2\Bigg[p^2\Big(6\nu(1-e^2)^3-15(1-e^2)^3\Big) - 72p(1-e^2)^2 + 72(1-e^2)
$$

$$+\sqrt{1-e^2}\bigg(p\bigg(\bigg(\frac{160e^2}{7}+\frac{50}{7}\bigg)\nu(1-e^2)+\bigg(\frac{352}{7}-\frac{401e^2}{7}\bigg)(1-e^2)\bigg)+36(1-e^2)+36\bigg)\bigg]\mathrm{J}^{(1)}_{pp0}-36p^3(1-e^2)^{3/2}\mathrm{J}^{(2)}_{pp0}$$

$$+p^2(1-e^2)\bigg[\frac{227\nu}{7}+\bigg(\frac{\nu^2}{8}-\frac{15\nu}{8}\bigg)p^2(1-e^2)^3+\bigg(-\frac{30\nu}{7}-\frac{242}{7}\bigg)p(1-e^2)^2+\bigg(\frac{37\nu^2}{42}-\frac{589\nu}{63}+\frac{97}{14}\bigg)(1-e^2)^2$$

$$+\bigg(-\frac{725\nu^2}{252}-\frac{6829\nu}{252}+\frac{14459}{252}\bigg)(1-e^2)+\frac{279}{7}+\sqrt{1-e^2}\bigg[18\nu+p\bigg(\bigg(\frac{73\nu^2}{189}-\frac{673\nu}{189}+\frac{7547}{756}\bigg)(1-e^2)^2$$

$$+\bigg(\frac{64\nu^2}{189}+\frac{3272\nu}{189}+\frac{53}{189}\bigg)(1-e^2)\bigg)+\bigg(\frac{785}{7}-\frac{192\nu}{7}\bigg)(1-e^2)-13\bigg]\bigg]\mathrm{J}^{(0)}_{pp1}+p^2(1-e^2)\bigg[\frac{216\nu}{7}$$

$$+\bigg(\frac{403}{7}-\frac{166\nu}{7}\bigg)(1-e^2)-\frac{555}{7}+\sqrt{1-e^2}\bigg[\bigg(\frac{30\nu}{7}-\frac{353}{7}\bigg)p(1-e^2)-72\bigg]\bigg]\mathrm{J}^{(1)}_{pp1}-36p^2(1-e^2)\mathrm{J}^{(2)}_{pp1}$$

$$+p^2(1-e^2)^2\bigg[-\frac{3\nu^2}{8}+\frac{4043\nu}{56}+\bigg(\frac{12\nu}{7}-\frac{4}{7}\bigg)p(1-e^2)^2+\bigg(-\frac{19\nu^2}{72}+\frac{1271\nu}{504}+\frac{41}{36}\bigg)(1-e^2)^2+\bigg(\frac{772\nu^2}{189}$$

$$-\frac{5140\nu}{189}+\frac{28838}{189}\bigg)(1-e^2)-\frac{1923}{14}+\sqrt{1-e^2}\bigg[-\frac{36\nu}{7}+p\bigg(\bigg(\frac{11\nu^2}{63}+\frac{113\nu}{63}-\frac{137}{252}\bigg)(1-e^2)^2$$

$$+\bigg(-\frac{64\nu^2}{189}-\frac{5\nu}{189}-\frac{13435}{378}\bigg)(1-e^2)\bigg)+\bigg(\frac{138\nu}{7}-\frac{424}{7}\bigg)(1-e^2)-\frac{1724}{7}\bigg]\bigg]\mathrm{J}^{(0)}_{pp2}+p^2(1-e^2)^2\bigg[-\frac{216\nu}{7}$$

$$+\bigg(\frac{142\nu}{7}-\frac{395}{7}\bigg)(1-e^2)-\frac{957}{7}+\sqrt{1-e^2}\bigg[\bigg(\frac{101}{7}-\frac{30\nu}{7}\bigg)p(1-e^2)+72\bigg]\bigg]\mathrm{J}^{(1)}_{pp2}+36p^2(1-e^2)^2\mathrm{J}^{(2)}_{pp2}$$

$$+p^2(1-e^2)^3\bigg[-\frac{1283\nu^2}{378}-\frac{14767\nu}{378}+\bigg(-\frac{\nu^2}{21}+\frac{1238\nu}{63}-\frac{659}{24}\bigg)(1-e^2)-\frac{19819}{216}+\sqrt{1-e^2}\bigg[\bigg(-\frac{265\nu^2}{189}-\frac{353\nu}{189}$$

$$+\frac{2707}{756}\bigg)p(1-e^2)+98\bigg]\bigg]\mathrm{J}^{(0)}_{pp3}+p^2(1-e^2)^3\bigg(\frac{60\nu}{7}+\frac{484}{7}\bigg)\mathrm{J}^{(1)}_{pp3}+p^2(1-e^2)^4\bigg[\frac{2\nu^2}{189}-\frac{3986\nu}{189}+\bigg(-\frac{331\nu^2}{126}$$

$$-\frac{1193\nu}{126}+\frac{211}{72}\bigg)(1-e^2)+\frac{16001}{216}+\sqrt{1-e^2}\bigg[-\frac{36\nu}{7}+\bigg(\frac{53\nu^2}{63}+\frac{103\nu}{63}-\frac{131}{252}\bigg)p(1-e^2)+\frac{12}{7}\bigg]\bigg]\mathrm{J}^{(0)}_{pp4}$$

$$+p^2(1-e^2)^4\bigg(\frac{12}{7}-\frac{36\nu}{7}\bigg)\mathrm{J}^{(1)}_{pp4}+p^2(1-e^2)^5\bigg(\frac{238\nu^2}{27}+\frac{5792\nu}{189}-\frac{12793}{756}\bigg)\mathrm{J}^{(0)}_{pp5}+p^2(1-e^2)^6\bigg(-\frac{265\nu^2}{63}$$

$$-\frac{515\nu}{63}+\frac{655}{252}\bigg)\mathrm{J}^{(0)}_{pp6}+e\bigg[p^3\bigg(\bigg(\frac{\nu^2}{8}-\frac{15\nu}{8}\bigg)(1-e^2)^3+\bigg(\frac{\nu^2}{8}-\frac{15\nu}{8}\bigg)(1-e^2)^2\bigg)+p^2\bigg(-27\nu$$

$$+\bigg(\frac{88\nu}{7}-\frac{313}{14}\bigg)(1-e^2)^2+\bigg(\frac{95\nu}{7}-\frac{1119}{7}\bigg)(1-e^2)+\frac{81}{2}\bigg)+p(54(1-e^2)+54)+\sqrt{1-e^2}\bigg[p^2\bigg(-\nu^2+25\nu$$

$$+\bigg(\frac{5\nu^2}{12}+\frac{15\nu}{28}-\frac{85}{84}\bigg)(1-e^2)^2+\bigg(\frac{74\nu^2}{21}-\frac{563\nu}{21}+\frac{585}{14}\bigg)(1-e^2)-\frac{101}{2}\bigg)+p\bigg(-42\nu+\bigg(\frac{232\nu}{7}-\frac{579}{7}\bigg)(1-e^2)+33\bigg)$$

$$+72\bigg]\bigg]J_{p-1}(ep)+\bigg[\bigg(\frac{15\nu}{4}-\frac{\nu^2}{4}\bigg)p^4(1-e^2)^3+p^3\bigg(\bigg(-\frac{\nu^2}{8}-\frac{1143\nu}{56}+\frac{430}{7}\bigg)(1-e^2)^3$$

$$+\bigg(-\frac{\nu^2}{8}+\frac{825\nu}{56}+\frac{768}{7}\bigg)(1-e^2)^2\bigg)+p^2\bigg(18\nu+\bigg(\frac{3\nu^2}{56}+\frac{37\nu}{24}-\frac{155}{168}\bigg)(1-e^2)^3+\bigg(-\frac{503\nu^2}{168}+\frac{1881\nu}{56}$$

$$-\frac{12203}{168}\bigg)(1-e^2)^2+\bigg(\frac{1927}{7}-\frac{419\nu}{7}\bigg)(1-e^2)-28\bigg)+p\bigg(27\nu+\bigg(\frac{243}{14}-\frac{74\nu}{7}\bigg)(1-e^2)^2+\bigg(\frac{132}{7}-\frac{53\nu}{7}\bigg)(1-e^2)$$

$$-\frac{189}{2}\bigg)-36(1-e^2)-36+\sqrt{1-e^2}\bigg[p^3\bigg(\bigg(-\frac{149\nu^2}{252}+\frac{317\nu}{84}-\frac{295}{252}\bigg)(1-e^2)^3+\bigg(-\frac{19\nu^2}{21}-\frac{709\nu}{126}-\frac{99}{2}\bigg)(1-e^2)^2$$

$$+\bigg(-\nu^2-\frac{74\nu}{21}+\frac{4415}{42}\bigg)(1-e^2)\bigg)+p^2\bigg(\nu^2-25\nu+\bigg(-\frac{5\nu^2}{12}-\frac{247\nu}{28}+\frac{1801}{84}\bigg)(1-e^2)^2+\bigg(-\frac{74\nu^2}{21}+\frac{605\nu}{21}$$

$$
\begin{aligned}
&+\frac{409}{14}\Big)(1-e^2)+\frac{245}{2}\Big)+p\Big(42\nu+\Big(\frac{327}{7}-\frac{232\nu}{7}\Big)(1-e^2)-105\Big)-72\Big]\Big]J_p(ep)+ep^2(1-e^2)\Big[-\frac{53\nu}{7}\\
&+\Big(\frac{243}{14}-\frac{74\nu}{7}\Big)(1-e^2)+\frac{27\nu-\frac{81}{2}}{(1-e^2)}+\frac{510}{7}+p\sqrt{1-e^2}\Big(3\nu+\Big(3\nu-\frac{15}{2}\Big)(1-e^2)-\frac{15}{2}\Big)\Big]{}^{(+)}\mathrm{J}^{(1,1)}_{pp0}\\
&-18ep^2(2-e^2){}^{(+)}\mathrm{J}^{(2,1)}_{pp0}+36e^2p^2\sqrt{1-e^2}{}^{(+)}\mathrm{J}^{(1,2)}_{pp0}+ep^2\Big[(6\nu-15)p(1-e^2)^2+\sqrt{1-e^2}\Big[42\nu+\Big(\frac{579}{7}-\frac{232\nu}{7}\Big)(1-e^2)\\
&-33\Big]\Big]{}^{(-)}\mathrm{J}^{(1,1)}_{pp0}-36ep^2{}^{(-)}\mathrm{J}^{(2,1)}_{pp0}+ep^2\Big[p\Big(\Big(\frac{\nu^2}{8}-\frac{15\nu}{8}\Big)(1-e^2)^3+\Big(\frac{\nu^2}{8}-\frac{15\nu}{8}\Big)(1-e^2)^2\Big)+\Big(\frac{403}{7}-\frac{166\nu}{7}\Big)(1-e^2)^2\\
&+\Big(\frac{216\nu}{7}-\frac{555}{7}\Big)(1-e^2)+\sqrt{1-e^2}\Big[27\nu+\Big(\frac{243}{14}-\frac{74\nu}{7}\Big)(1-e^2)^2+\Big(\frac{6}{7}-\frac{53\nu}{7}\Big)(1-e^2)-\frac{81}{2}\Big]\Big]{}^{(-)}\mathrm{J}^{(0,1)}_{pp1}\\
&-36ep^2\Big[2(1-e^2)+\sqrt{1-e^2}(2-e^2)\Big]{}^{(-)}\mathrm{J}^{(1,1)}_{pp1}-18e^2p^2(2-e^2){}^{(-)}\mathrm{J}^{(1,2)}_{pp0}\Big\}
\end{aligned}
\tag{92}
$$

C. Comparison with post-circular expansion

Building on the preceding results, one can compute GWs from binary systems with arbitrary eccentricity directly by following the procedure outlined in Section II. [51] shows that as the eccentricity increases, the number of Fourier modes required for a high-fidelity waveform rises steeply; when the eccentricity approaches 0.9, hundreds of modes are needed. Although we have introduced methods and tools for evaluating high-order PN contributions, waveform generation remains time-consuming at large eccentricities, so there is still substantial scope for optimization. In the remainder of this section we present several illustrative examples to demonstrate why the new method is indispensable in the high-eccentricity regime.

First, we compute the 3PN orbital dynamical variables $(\bar{v}, \bar{e}, \bar{l}, \bar{\lambda}, \bar{\chi})$ together with the post-adiabatic corrections $(\tilde{v}, \tilde{e}, \tilde{l}, \tilde{\lambda})$ as described in Section II. We then obtain the 3PN waveform by summing $H_{\ell m} = \sum_p H_{\ell(-m)p}, \mathrm{e}^{\mathrm{i}pl}$ until the desired accuracy is achieved. For comparison, we also use the familiar post-circular expansion truncated at $\mathcal{O}\big(e^{10}\big)$.

Figures (1)-(3) plot the leading harmonic $h_{\ell\ell}$ of the first four multipoles for three representative cases with symmetric mass ratio $\nu = 0.22$, initial frequency $v_0 = 0.25$, and initial eccentricities of 0.3, 0.4, and 0.5.

Figure (1) indicates that for $e \sim 0.3$ the post-circular expansion up to $\mathcal{O}\big(e^{10}\big)$ is reasonably reliable. However, its accuracy degrades rapidly as the eccentricity grows. At $e \sim 0.4$, higher multipoles with $\ell > 3$ already break down; by $e \sim 0.5$, errors during the early, highly eccentric inspiral exceed the waveform amplitude itself. These findings make it clear that for moderately eccentric orbits the post-circular approach struggles to describe high-order multipole waveforms accurately. Developing faster and more precise frequency-domain techniques for waveform generation therefore remains a pressing challenge.

IV. RE-EXPRESSION OF TAIL EFFECTS IN GW FLUXES

The GW energy flux is consist of instantaneous part, which is directly determined by the dynamics of the source, and hereditary part, which is caused by non-linear interactions. The reason for the nonlinear effect is the interaction between the radiative moments and the source-type moments or themselves. Formally these hereditary part are expressed as integrals. These genetic terms can be divided into a tail part and a memory part. The former originates from the interaction related to the radiative moments, while the latter originates from the change of the radiative moment. Sometimes the memory part is also classified as the instantaneous part [90], while the energy flux would becomes instantaneous after taking a time derivative and the angular momentum would be hereditary [85].

Generally, the energy and angular momentum fluxes of GW read [71]

$$
\mathcal{F} = \sum_{\ell\geq 2} \frac{1}{c^{2\ell+1}}\Big[a_\ell U_L^{(1)} U_L^{(1)} + \frac{1}{c^2} b_\ell V_L^{(1)} V_L^{(1)}\Big], \tag{93}
$$

$$
\mathcal{G}^i = \epsilon_{iab} \sum_{\ell\geq 2} \frac{1}{c^{2\ell+1}}\Big[\tilde{a}_\ell U_{a(L-1)} U_{b(L-1)}^{(1)} + \frac{1}{c^2}\tilde{b}_\ell V_{a(L-1)} V_{b(L-1)}^{(1)}\Big], \tag{94}
$$

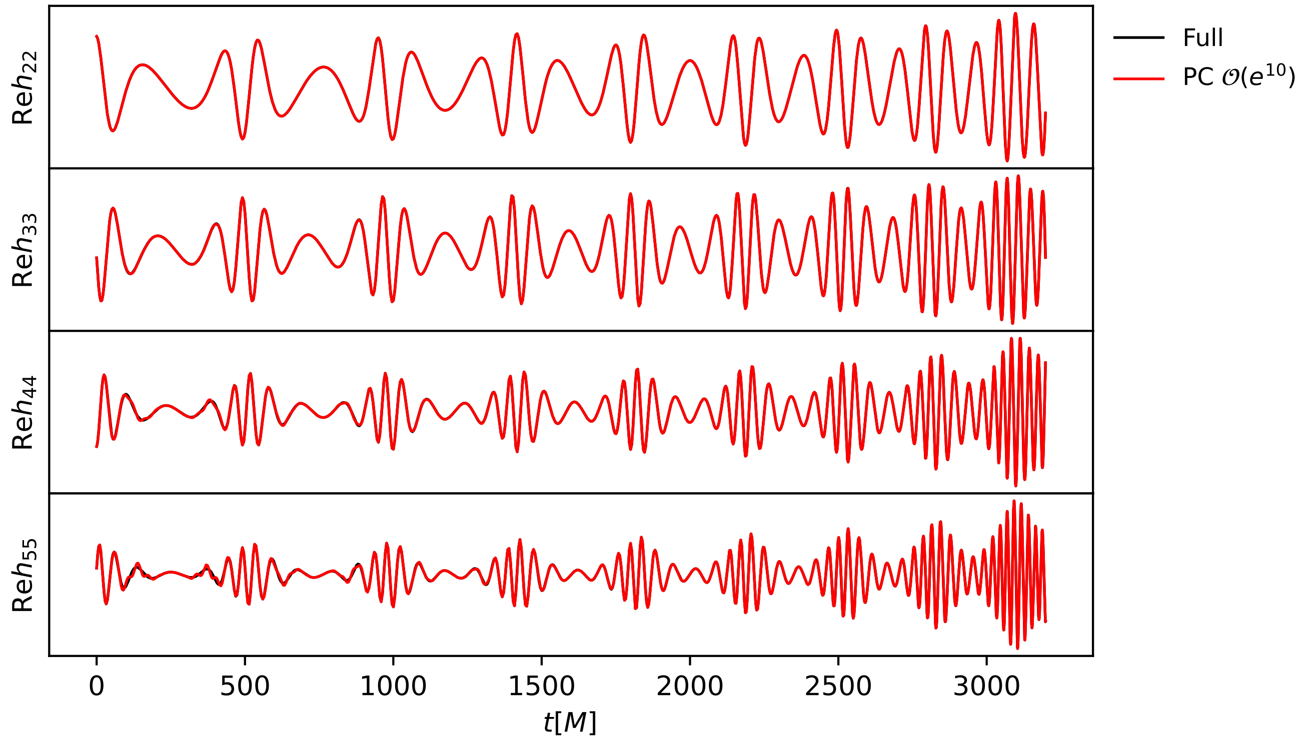

FIG. 1: Comparison of the leading-mode waveforms $h_{\ell\ell}$ (first four multipoles up to 3PN) computed with the Fourier-mode expansion and the post-circular expansion. In this example the binary has mass ratio $\nu = 0.22$, initial frequency $v_0 = 0.25$, and the evolution ends at $v = 1/\sqrt{6}$. The initial eccentricity is $e_0 = 0.3$. The black curve corresponds to the Fourier-mode approach presented in this paper, obtained by summing $H_{\ell m} = \sum_p H_{\ell(-m)p} \mathrm{e}^{\mathrm{i}pl}$ until the required accuracy is reached; the red curve shows the post-circular waveform truncated at $\mathcal{O}\big(e^{10}\big)$.

where

$$a_\ell = \frac{(\ell+1)(\ell+2)}{\ell(\ell-1)\ell!(2\ell+1)!!}, \; b_\ell = \frac{4\ell(\ell+2)}{(\ell-1)(\ell+1)!(2\ell+1)!!}, \tag{95}$$

$$\tilde{a}_\ell = \frac{(\ell+1)(\ell+2)}{(\ell-1)\ell!(2\ell+1)!!}, \; \tilde{b}_\ell = \frac{4\ell^2(\ell+2)}{(\ell-1)(\ell+1)!(2\ell+1)!!} \tag{96}$$

Up to 4PN, the radiative moments U_L takes the form [97, 98],

$$\begin{aligned} U_L = {}& M_L^{(\ell)} + \frac{1}{c^3} U_L^{\mathrm{tail}} + \frac{1}{c^5}\Big(U_L^{\mathrm{mem},2.5\mathrm{PN}} + U_L^{M^2,2.5\mathrm{PN}}\Big) + \frac{1}{c^6} U_L^{\mathrm{tail(tail)}} + \frac{1}{c^7}\Big(U_L^{\mathrm{mem},3.5\mathrm{PN}} + U_L^{M^2,3.5\mathrm{PN}}\Big) \\ &+ \frac{1}{c^8} U_L^{\mathrm{tail(mem)}} + \mathcal{O}\big(c^{-9}\big) \end{aligned} \tag{97}$$

And similar for V_L. The 4.5PN tail-of-tail-of-tail contribution to canonical moments were known [99]. All of these tail terms involve infinite integrals over logarithms. The usual procedure is to insert the Fourier expansion of the multipole moments and then average over the orbit. In this way, the contribution of the tails to the flux can be written in terms of several eccentricity-enhancement functions. In this section, we follow the method of [52] and, together with the new J-integrals introduced in this paper, express these eccentricity-enhancement functions as sums of these J-integrals. We introduce

$$\mathcal{M}_\ell^{\mathcal{F}}(0) = M_L^{(\ell+1)} \int_0^\infty \mathrm{d}\tau M_L^{(\ell+3)}(t_r - \tau)\Big(\ln\tau + \kappa_0^{(\ell,0)}\Big), \tag{98}$$

$$\mathcal{M}_\ell^{\mathcal{F}}(\alpha) = 2M_L^{(\ell+1)} \int_0^\infty \mathrm{d}\tau M_L^{(\ell+\alpha+3)}(t_r - \tau) \sum_{s=0}^{\alpha+1} \kappa_s^{(\ell,\alpha)} \ln^s\tau + \sum_{j=0}^{\alpha-1}\left(\int_0^\infty \mathrm{d}\tau M_L^{(\ell+j+3)} \sum_{s_1=0}^{j+1} \kappa_{s_1}^{(\ell,j)} \ln^{s_1}\tau\right)$$

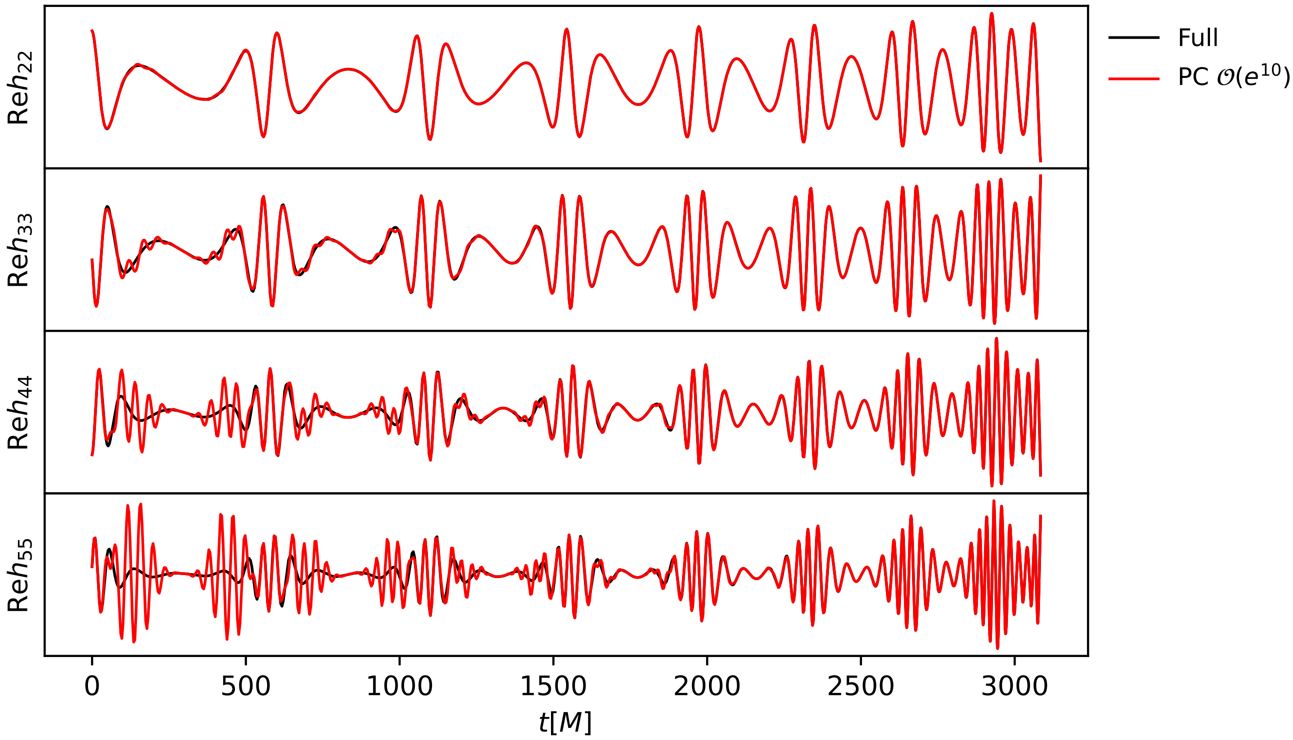

FIG. 2: Comparison of the leading-mode waveforms $h_{\ell\ell}$ (first four multipoles up to 3PN) computed with the Fourier-mode expansion and the post-circular expansion. In this example the binary has mass ratio $\nu = 0.22$, initial frequency $v_0 = 0.25$, and the evolution ends at $v = 1/\sqrt{6}$. The initial eccentricity is $e_0 = 0.4$. The black curve corresponds to the Fourier-mode approach presented in this paper, obtained by summing $H_{\ell m} = \sum_p H_{\ell(-m)p} \mathrm{e}^{\mathrm{i}pl}$ until the required accuracy is reached; the red curve shows the post-circular waveform truncated at $\mathcal{O}\big(e^{10}\big)$.

$$\times\left(\int_0^\infty \mathrm{d}\tau\mathrm{d}\tau M_L^{(\ell+\alpha-j+2)} \sum_{s_2=0}^{\alpha-j} \kappa_{s_2}^{(\ell,\alpha-j-1)} \ln^{s_2}\tau\right) \tag{99}$$

$$\mathcal{M}_\ell^{\mathcal{G}}(0) = \epsilon_{zab}\left[M_{a(L-1)}^{(\ell)} \int_0^\infty \mathrm{d}\tau M_{b(L-1)}^{(\ell+3)}(t_r-\tau)\Big(\ln\tau + \kappa_0^{(\ell,0)}\Big) + M_{b(L-1)}^{(\ell+1)} \int_0^\infty \mathrm{d}\tau M_{a(L-1)}^{(\ell+2)}(t_r-\tau)\Big(\ln\tau + \kappa_0^{(\ell,0)}\Big)\right], \tag{100}$$

$$\begin{aligned}\mathcal{M}_\ell^{\mathcal{G}}(\alpha) = \epsilon_{zab}&\Bigg[M_{a(L-1)}^{(\ell)} \int_0^\infty \mathrm{d}\tau M_{b(L-1)}^{(\ell+\alpha+3)} \sum_{s=0}^{\alpha+1} \kappa_s^{(\ell,\alpha)} \ln^s\tau + M_{b(L-1)}^{(\ell+1)} \int_0^\infty \mathrm{d}\tau M_{a(L-1)}^{(\ell+\alpha+2)} \sum_{s=0}^{\alpha+1} \kappa_s^{(\ell,\alpha)} \ln^s\tau \\ &+ \sum_{j=0}^{\alpha-1}\left(\int_0^\infty \mathrm{d}\tau M_{a(L-1)}^{(\ell+j+2)} \sum_{s_1=0}^{j+1} \kappa_{s_1}^{(\ell,j)} \ln^{s_1}\tau\right)\left(\int_0^\infty \mathrm{d}\tau M_{b(L-1)}^{(\ell+\alpha-j+2)} \sum_{s_2=0}^{\alpha-j} \kappa_{s_2}^{(\ell,\alpha-j-1)} \ln^{s_2}\tau\right)\Bigg]\end{aligned} \tag{101}$$

where $\kappa_s^{(\ell,\alpha)}$ are constants. These integrals will appear in the tail-related calculations. The structure of the contribution part of moment S_L is the same, just replace M_L with S_L and the associated constants $\kappa_s^{(\ell,n)}$. We currently do not consider the effects of radiation reactions on these moment derivatives, keeping on adiabatic approximation and neglect possible dissipative pieces [100]. And nor more complicated moment interactions, such as tail-memory terms. Substituting Fourier expansion of M_L, and average over ℓ, one would get the following summation

$$\sum_{p,p',m,m'} \mathrm{i}^{a+b}(pn+mv^3)^a(p'n+m'v^3)^b \underset{(p,m)}{\mathrm{M}_L}\ \underset{(p',m')}{\mathrm{M}_L} \left\langle \mathrm{e}^{\mathrm{i}[(p+p')l+(m+m')\lambda]}\right\rangle \int_0^\infty \mathrm{e}^{-\mathrm{i}(p'+m'(k+1))n\tau}\left(\sum_s \kappa_s^{(\ell,\alpha)} \ln^s\tau\right)\mathrm{d}\tau\,. \tag{102}$$

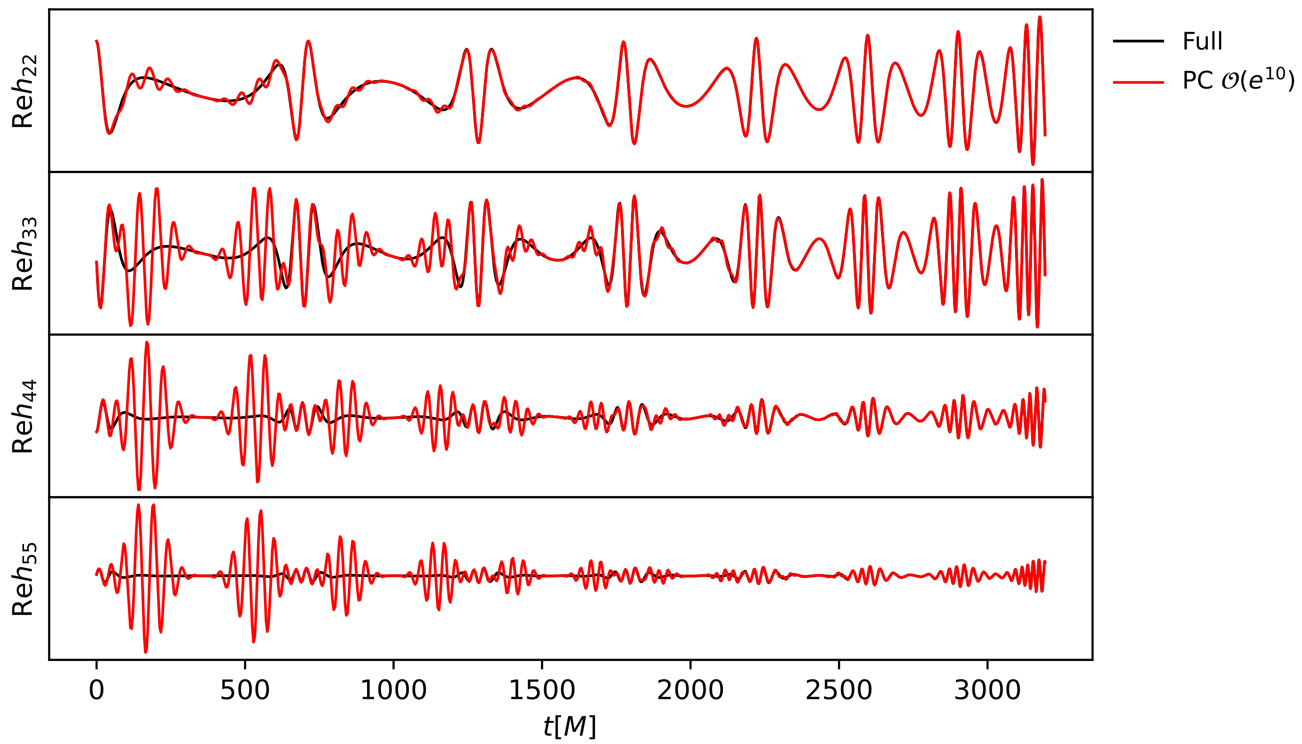

FIG. 3: Comparison of the leading-mode waveforms $h_{\ell\ell}$ (first four multipoles up to 3PN) computed with the Fourier-mode expansion and the post-circular expansion. In this example the binary has mass ratio $\nu = 0.22$, initial frequency $v_0 = 0.25$, and the evolution ends at $v = 1/\sqrt{6}$. The initial eccentricity is $e_0 = 0.5$. The black curve corresponds to the Fourier-mode approach presented in this paper, obtained by summing $H_{\ell m} = \sum_p H_{\ell(-m)p} \mathrm{e}^{\mathrm{i}pl}$ until the required accuracy is reached; the red curve shows the post-circular waveform truncated at $\mathcal{O}\big(e^{10}\big)$.

The average over l reads

$$\left\langle \mathrm{e}^{\mathrm{i}\left(p+p'+m+m'+(m+m')k\right)l} \right\rangle := \frac{1}{2\pi}\int_0^{2\pi} \mathrm{e}^{\mathrm{i}\left(p+p'+m+m'+(m+m')k\right)l}\,\mathrm{d}l$$
$$= \delta_{(p+p'+m+m')0} + \begin{cases} \displaystyle\sum_{j=1}^{\infty} \frac{\big(\mathrm{i}2\pi k(m+m')\big)^j}{(j+1)!} = \mathrm{i}k(m+m')\pi + \mathcal{O}\big(k^2\big) & p+p'+m+m'=0 \\ \displaystyle\sum_{j=1}^{\infty}\sum_{j'=0}^{j-1} \frac{(-1)^{j'}\big(\mathrm{i}2\pi k(m+m')\big)^j}{(j-j')!\big(\mathrm{i}2\pi(p+p'+m+m')\big)^{j'+1}} = \frac{k(m+m')}{p+p'+m+m'} + \mathcal{O}\big(k^2\big) & p+p'+m+m' \neq 0 \end{cases} \tag{103}$$

Note that averaging the l here does not seem to completely limit the Fourier mode index $p+p'+m+m'$, but we find that in fact the higher PN order part still vanishes. This is because of the factor $(m+m')^j$ would cancel the summation,

$$\sum_{m,m'} (m+m')^j m^a m'^b \underset{(p-m,m)}{\mathrm{M}_L} \underset{(p'-m',m')}{\mathrm{M}_L} = 0, \tag{104}$$

$$\sum_{m,m'} (m+m')^j m^a m'^b \underset{(p-m,m)}{\mathrm{S}_L} \underset{(p'-m',m')}{\mathrm{S}_L} = 0, \tag{105}$$

$$\epsilon_{zab} \sum_{m,m'} (m+m')^j m^a m'^b \underset{(p-m,m)}{\mathrm{M}_{a(L-1)}} \underset{(p'-m',m')}{\mathrm{M}_{b(L-1)}} = 0, \tag{106}$$

$$\epsilon_{zab} \sum_{m,m'} (m+m')^j m^a m'^b \underset{(p-m,m)}{\mathrm{S}_{a(L-1)}} \underset{(p'-m',m')}{\mathrm{S}_{b(L-1)}} = 0. \tag{107}$$

The 1PN property was shown in [83]. By inserting the Fourier modes of all the 3PN multipole moments we computed, it is easy to verify that they all hold for any positive j and any non-negative a, b. This is not a coincidence; it is very likely true for higher PN orders as well. When j is even, this can be proved using the symmetry of STF tensors; when j is odd, it should involve properties of the Einstein field equations themselves. Although we cannot prove it for all PN orders here, even restricting ourselves to the 3PN multipole moments M_L, S_L greatly simplifies the final result. We define the following auxiliary symbols for simplification,

$$\underset{(p)}{\mathrm{M}_L} := \sum_{m=-\ell}^{\ell} \underset{(p-m,m)}{\mathrm{M}_L}, \tag{108}$$

$$\left[{}_{(s)}\underset{(p)}{\mathrm{M}_L}\right] := \sum_{m=-\ell}^{\ell} m^s \underset{(p-m,m)}{\mathrm{M}_L}. \tag{109}$$

Eq. (104)-(107) tells us

$$\sum_{s=0}^{j} (-1)^{j-s+b} \binom{j}{s} \left[{}_{(s+a)}\underset{(p)}{\mathrm{M}_L}\right] \left[{}_{(j-s+b)}\underset{(p')}{\mathrm{M}^*_L}\right] = 0, \tag{110}$$

$$\epsilon_{zab} \sum_{s=0}^{j} (-1)^{j-s+b} \binom{j}{s} \left[{}_{(s+a)}\underset{(p)}{\mathrm{M}_{a(L-1)}}\right] \left[{}_{(j-s+b)}\underset{(p')}{\mathrm{M}^*_{a(L-1)}}\right] = 0. \tag{111}$$

Therefore one can expand Eq. (102), and rewrite it by $\underset{(p)}{\mathrm{M}_L}$ and $\left[{}_{(s)}\underset{(p)}{\mathrm{M}_L}\right]$. First, let's consider the simplest cases $\mathcal{M}^{\mathcal{F}}_{\ell}(0), \mathcal{M}^{\mathcal{G}}_{\ell}(0)$. Following the above steps and then sorting them out, we find they can be re-summed as very simple forms

$$\mathcal{M}^{\mathcal{F}}_{\ell}(0) = \frac{\pi}{n} \sum_{p=1}^{\infty} \underset{(p)}{\mathbb{M}_L} \underset{(p)}{\mathrm{M}^*_L}, \tag{112}$$

$$\mathcal{M}^{\mathcal{G}}_{\ell}(0) = -\frac{\mathrm{i}\pi}{n} \epsilon_{zab} \sum_{p=1}^{\infty} \underset{(p)}{\tilde{\mathbb{M}}_{a(L-1)}} \underset{(p)}{\mathrm{M}^*_{b(L-1)}}, \tag{113}$$

where

$$\underset{(p)}{\mathbb{M}_L} := \sum_{m=-\ell}^{\ell} \frac{\left[(p-m)n + mv^3\right]^{2(\ell+2)}}{p+mk} \underset{(p-m,m)}{\mathrm{M}_L}, \tag{114}$$

$$\underset{(p)}{\tilde{\mathbb{M}}_L} := \sum_{m=-\ell}^{\ell} \frac{\left[(p-m)n + mv^3\right]^{2\ell+3}}{p+mk} \underset{(p-m,m)}{\mathrm{M}_L}. \tag{115}$$

And we emphasize here $n = \dot{l}$. Similarly, the higher order cases $\mathcal{M}^{\mathcal{F}}_{\ell}(\alpha), \mathcal{M}^{\mathcal{G}}_{\ell}(\alpha)$ are

$$\mathcal{M}^{\mathcal{F}}_{\ell}(\alpha) = \frac{\pi}{n} \sum_{p=1}^{\infty} \left[{}_{(\alpha)}\underset{(p)}{\mathbb{M}_L}\right] \underset{(p)}{\mathrm{M}^*_L}, \tag{116}$$

$$\mathcal{M}^{\mathcal{G}}_{\ell}(\alpha) = -\frac{\mathrm{i}\pi}{n} \epsilon_{zab} \sum_{p=1}^{\infty} \left[{}_{(\alpha)}\underset{(p)}{\tilde{\mathbb{M}}_{a(L-1)}}\right] \underset{(p)}{\mathrm{M}^*_{b(L-1)}}, \tag{117}$$

where

$$\left[{}_{(\alpha)}\underset{(p)}{\mathbb{M}_L}\right] := \sum_{m=-\ell}^{\ell} \frac{\left[(p-m)n + mv^3\right]^{2(\ell+2)+\alpha}}{p+mk} \Lambda^{(M)}_{\ell p m \alpha} \underset{(p-m,m)}{\mathrm{M}_L}, \tag{118}$$

$$\left[{}_{(\alpha)}\underset{(p)}{\tilde{\mathbb{M}}_L}\right] := \sum_{m=-\ell}^{\ell} \frac{\left[(p-m)n + mv^3\right]^{2\ell+3+\alpha}}{p+mk} \Lambda^{(M)}_{\ell p m \alpha} \underset{(p-m,m)}{\mathrm{M}_L}, \tag{119}$$

$$\Lambda^{(M)}_{\ell pm\alpha} = \frac{\mathrm{i}^{\alpha+1}}{2\pi}\Bigg[\sum_{s=0}^{\alpha+1}\kappa_s^{(l,\alpha)}\Big(\Lambda^{(+)}_{pms} - (-1)^\alpha\Lambda^{(-)}_{pms}\Big) - \frac{(p-m)n + mv^3}{2n(p+mk)}\sum_{j=0}^{\alpha-1}\sum_{s_1}^{j+1}\sum_{s_2=0}^{\alpha-j}(-1)^j\kappa_{s_1}^{(\ell,j)}\kappa_{s_2}^{(l,\alpha-j-1)}$$
$$\times\Big(\Lambda^{(-)}_{pms_1}\Lambda^{(+)}_{pms_2} - (-1)^\alpha\Lambda^{(+)}_{pms_1}\Lambda^{(-)}_{pms_2}\Big)\Bigg], \tag{120}$$

$$\Lambda^{(\pm)}_{pms} := \sum_{s'=0}^{s}\binom{s}{s'}\bar{\boldsymbol{\gamma}}_{s-s'}\ln^{s'}\big(\pm\mathrm{i}n(p+mk)\big). \tag{121}$$

We denote $\Lambda_{\ell pm0} = 1$, then formally $\big[_{(0)}\underset{(p)}{\mathbb{M}_L}\big] = \underset{(p)}{\mathbb{M}_L}$. The expression for the moment S_L takes the same structure, one just need to replace the constant symbol $\kappa_s^{(\ell,j)}$ with $\pi_s^{(\ell,j)}$. These results reproduce the work of [52, 101]. For example, when $\ell = 2$,

$$\langle\mathcal{F}_{\text{tail,quad}}\rangle = a_\ell\Big(4M_{\text{ADM}}\mathcal{M}_2^{\mathcal{F}}(0) + M^2_{\text{ADM}}\mathcal{M}_2^{\mathcal{F}}(1)\Big) = \frac{32v^{13}\nu^2}{5}\Bigg[4\pi\varphi(e) + \pi v^2\Big(-\frac{428}{21}\alpha(e) + \frac{178}{21}\nu\theta(e)\Big)$$
$$+ v^3\Bigg(\bigg(-\frac{515063}{11025} + \frac{16\pi^2}{3} - \frac{856}{35}\ln\Big(\frac{v^2}{x_0'}\Big)\bigg)F(e) - \frac{1712}{105}\chi(e)\Bigg) + \mathcal{O}\big(c^{-4}\big)\Bigg] \tag{122}$$

$$\langle\mathcal{G}^z_{\text{tail,quad}}\rangle = \tilde{a}_\ell\Big(4M_{\text{ADM}}\mathcal{M}_2^{\mathcal{G}}(0) + M^2_{\text{ADM}}\mathcal{M}_2^{\mathcal{G}}(1)\Big) = \frac{32v^{10}\nu^2}{5}\Bigg[4\pi\tilde{\varphi}(e) + \pi v^2\Big(-\frac{428}{21}\tilde{\alpha}(e) + \frac{178}{21}\nu\tilde{\theta}(e)\Big)$$
$$+ v^3\Bigg(\bigg(-\frac{515063}{11025} + \frac{16\pi^2}{3} - \frac{856}{35}\ln\Big(\frac{v^2}{x_0'}\Big)\bigg)\tilde{F}(e) - \frac{1712}{105}\tilde{\chi}(e)\Bigg) + \mathcal{O}\big(c^{-4}\big)\Bigg]. \tag{123}$$

The eccentricity enhancement function is defined by summing the product of the multipole moments,

$$\varphi(e) = \frac{v^8}{32\nu^2}\sum_{p=1}^{\infty}p^7\mathrm{PN}_0\Big[\underset{(p)}{\mathrm{M}_L}\,\underset{(p)}{\mathrm{M}^*_L}\Big], \qquad \tilde{\varphi}(e) = -\mathrm{i}\frac{v^8}{16\nu^2}\epsilon_{zab}\sum_{p=1}^{\infty}p^6\mathrm{PN}_0\Big[\underset{(p)}{\mathrm{M}_{a(L-1)}}\,\underset{(p)}{\mathrm{M}^*_{b(L-1)}}\Big], \tag{124}$$

$$F(e) = \frac{v^8}{64\nu^2}\sum_{p=1}^{\infty}p^8\mathrm{PN}_0\Big[\underset{(p)}{\mathrm{M}_L}\,\underset{(p)}{\mathrm{M}^*_L}\Big], \qquad \tilde{F}(e) = -\mathrm{i}\frac{v^8}{32\nu^2}\epsilon_{zab}\sum_{p=1}^{\infty}p^7\mathrm{PN}_0\Big[\underset{(p)}{\mathrm{M}_{a(L-1)}}\,\underset{(p)}{\mathrm{M}^*_{b(L-1)}}\Big], \tag{125}$$

$$\chi(e) = \frac{v^8}{64\nu^2}\sum_{p=1}^{\infty}p^8\ln\Big(\frac{p}{2}\Big)\mathrm{PN}_0\Big[\underset{(p)}{\mathrm{M}_L}\,\underset{(p)}{\mathrm{M}^*_L}\Big], \qquad \tilde{\chi}(e) = -\mathrm{i}\frac{v^8}{32\nu^2}\epsilon_{zab}\sum_{p=1}^{\infty}p^7\ln\Big(\frac{p}{2}\Big)\mathrm{PN}_0\Big[\underset{(p)}{\mathrm{M}_{a(L-1)}}\,\underset{(p)}{\mathrm{M}^*_{b(L-1)}}\Big]. \tag{126}$$

PN_a denotes taking $\mathcal{O}\big(c^{-2a}\big)$, the ath PN part. The explicit form of $\alpha(e), \tilde{\alpha}(e), \theta(e)$ and $\tilde{\theta}(e)$ are given by [83], here we reproduce them in terms of our convention

$$-\frac{428}{21}\alpha(e) + \frac{178}{21}\nu\theta(e) = 4\Big(\varphi_{(0,1)}(e) - \frac{1}{2}\nu\varphi(e) - \frac{21}{1-e^2}\big(\varphi(e) - \varphi_{(1,0)}(e)\big)\Big), \tag{127}$$

$$-\frac{428}{21}\tilde{\alpha}(e) + \frac{178}{21}\nu\tilde{\theta}(e) = 4\Big(\tilde{\varphi}_{(0,1)}(e) - \frac{1}{2}\nu\tilde{\varphi}(e) - \frac{18}{1-e^2}\big(\tilde{\varphi}(e) - \tilde{\varphi}_{(1,0)}(e)\big)\Big), \tag{128}$$

where

$$\varphi_{(a,b)}(e) := \frac{v^{8-2b}}{32\nu^2}\sum_{p=1}^{\infty}p^{7-a}\mathrm{PN}_b\Big[\big[_{(a)}\underset{(p)}{\mathrm{M}_L}\big]\,\underset{(p)}{\mathrm{M}^*_L}\Big], \tag{129}$$

$$\tilde{\varphi}_{(a,b)}(e) := -\mathrm{i}\frac{v^{8-2b}}{16\nu^2}\epsilon_{zij}\sum_{p=1}^{\infty}p^{6-a}\mathrm{PN}_b\Big[\big[_{(a)}\underset{(p)}{\mathrm{M}_{i(L-1)}}\big]\,\underset{(p)}{\mathrm{M}^*_{j(L-1)}}\Big]. \tag{130}$$

The reason for these symbols is that when $\underset{(p)}{\mathbb{M}_L}$ is expanded, one get

$$\underset{(p)}{\mathbb{M}_L} = p^{2\ell+3}v^{6(\ell+2)}\Bigg[\underset{(p)}{\mathrm{M}_L} + \frac{v^2}{1-e^2}\Big(3(2\ell+3)\big[_{(1)}\underset{(p)}{\mathrm{M}_L}\big] - 6(\ell+2)\underset{(p)}{\mathrm{M}_L}\Big) + \mathcal{O}\big(c^{-4}\big)\Bigg]. \tag{131}$$

Similarly, for higher-order tail integrals, the corresponding expansions of $\left[{}_{(\alpha)}\underset{(p)}{\mathbb{M}_L}\right]$ will also include similar terms. In our convention, these eccentricity enhancement functions can all be expressed as infinite sums of products of J-integrals. It is well known that some of these sums can be written in simple closed form,

$$F(e) = \frac{1}{(1-e^2)^{13/2}}\left(1 + \frac{85e^2}{6} + \frac{5171e^4}{192} + \frac{1751e^6}{192} + \frac{297e^8}{1024}\right), \tag{132}$$

$$\tilde{F}(e) = \frac{1}{(1-e^2)^5}\left(1 + \frac{229e^2}{32} + \frac{327e^4}{64} + \frac{69e^6}{256}\right). \tag{133}$$

Consider the general form of summation that appears in eccentricity enhancement function expressions: $\sum_p p^n \mathrm{J}^{(b_1)}_{(p+m_1)pa_1}\mathrm{J}^{(b_2)}_{(p+m_2)pa_2}$, a closed-form expression exists only when the summation is carried out over p from negative to positive infinity. Using the generating function method, this sum can be calculated as follows,

$$\sum_{p=-\infty}^{\infty} p^n \mathrm{J}^{(b_1)}_{(p+m_1)pa_1}\mathrm{J}^{(b_2)}_{(p+m_2)pa_2} = \frac{1}{2\pi}\int_{-\pi}^{\pi} \mathrm{i}^{b_1+b_2-n}\frac{\delta\chi(x)^{b_1}\mathrm{e}^{\mathrm{i}m_1 x}}{(1-e\cos x)^{a_1}}\frac{\partial^n}{\partial z^n}\left[\frac{\delta\chi(\sigma)^{b_2}\mathrm{e}^{\mathrm{i}m_2\sigma}}{(1-e\cos\sigma)^{a_2+1}}\right]\Bigg|_{z=0}\mathrm{d}x \tag{134}$$

where $\sigma(z,x)$ is an implicit function determined by,

$$x + \sigma(z,x) + z = e(\sin x + \sin\sigma(z,x)). \tag{135}$$

In addition, due to the symmetry of the dynamic structure itself, after tedious arrangement, it can be found that some eccentricity enhancement functions can be written in closed form. For example, one can obtain the following results which will appear in the next PN order of $\mathcal{M}_2^{\mathcal{F}}(1)$,

$$F_{(1,0)}(e) := \frac{v^8}{64\nu^2}\sum_{p=1}^{\infty} p^7 \mathrm{PN}_0\left[\left[{}_{(1)}\underset{(p)}{\mathrm{M}_L}\right]\underset{(p)}{\mathrm{M}^*_L}\right] = \frac{1}{(1-e^2)^5}\left(1 + \frac{229e^2}{32} + \frac{327e^4}{64} + \frac{69e^6}{256}\right) = \tilde{F}(e), \tag{136}$$

$$\tilde{F}_{(1,0)}(e) := -\mathrm{i}\frac{v^8}{32\nu^2}\epsilon_{zab}\sum_{p=1}^{\infty} p^6 \mathrm{PN}_0\left[\left[{}_{(1)}\underset{(p)}{\mathrm{M}_{a(L-1)}}\right]\underset{(p)}{\mathrm{M}^*_{b(L-1)}}\right] = \frac{1}{(1-e^2)^{7/2}}\left(1 + \frac{97}{32}e^2 + \frac{49}{128}e^4\right), \tag{137}$$

$$\begin{aligned} F_{(0,1)}(e) := \frac{v^8}{64\nu^2}\sum_{p=1}^{\infty} p^8 \mathrm{PN}_1\left[\underset{(p)}{\mathrm{M}_L}\,\underset{(p)}{\mathrm{M}^*_L}\right] &= -\frac{107}{21(1-e^2)^8}\Bigg[\frac{507}{107} + \frac{10395e^2}{428} - \frac{33075e^4}{856} - \frac{45045e^6}{3424} + \frac{36855e^8}{1712} + \frac{4347e^{10}}{3424} \\ &- \sqrt{1-e^2}\left(\frac{397}{107} + \frac{216615e^2}{3424} + + \frac{548117e^4}{3424} + \frac{616191e^6}{6848} + \frac{69631e^8}{6848} + \frac{43119e^{10}}{438272}\right)\Bigg] \\ &+ \frac{55\nu}{21(1-e^2)^{15/2}}\left(1 + \frac{3031e^2}{240} + \frac{60763e^4}{3520} - \frac{267e^6}{176} - \frac{67567e^8}{33792} - \frac{5427e^{10}}{112640}\right), \end{aligned} \tag{138}$$

$$\begin{aligned} \tilde{F}_{(0,1)}(e) := -\mathrm{i}\frac{v^8}{32\nu^2}\epsilon_{zab}\sum_{p=1}^{\infty} p^7 \mathrm{PN}_1\left[\underset{(p)}{\mathrm{M}_{a(L-1)}}\,\underset{(p)}{\mathrm{M}^*_{b(L-1)}}\right] &= -\frac{107}{21(1-e^2)^8}\Bigg[\sqrt{1-e^2}\left(\frac{441}{107} + \frac{28665e^2}{3424} - \frac{149499e^4}{13696}\right. \\ &\left. - \frac{21609e^6}{13696}\right) - \left(\frac{334}{107} + \frac{101779e^2}{3424} + \frac{483379e^4}{13696} + \frac{181765e^6}{27392} + \frac{20241e^8}{219136}\right)\Bigg] + \frac{55\nu}{21(1-e^2)^6}\left(1 + \frac{11483e^2}{1760} + \frac{2461e^4}{880}\right. \\ &\left. - \frac{963e^6}{1280} - \frac{1833e^8}{56320}\right) \end{aligned} \tag{139}$$

The above method is also applicable to the multipole moment S_L, which will not be elaborated here. At the end of this section, we emphasize that although we have, using the new tools developed in this paper, derived a general re-summed expression for the tail part flux without including other complicated interaction terms, this expression is valid only when the conditions in Eq. (104)-(107) are satisfied. Substituting the 3PN multipole-moment results, we find that the condition indeed holds; therefore, at least for the tail contribution to the flux through 4.5PN order under the adiabatic approximation, our expression is reliable. Whether higher-PN multipole moments continue to satisfy this condition remains to be established by a rigorous proof.

V. SUMMARY

With the rapid progress of GW observations and the planning of next-generation detectors, the demand for more accurate waveform templates has intensified. This paper introduces a new mathematical framework that compactly captures the dynamics of compact binaries and the high-order PN structure of their gravitational radiation. We also release a ready-to-use software package implementing the method. We then apply the framework to the computation of the tail contribution to binary waveforms and derive a highly general re-summed expression. This result streamlines the evaluation of tail terms in the fluxes at higher PN orders.

At present, our treatment is restricted to non-spinning binaries. The inclusion of spins renders the Fourier structure substantially more intricate; extending the method to generic spinning, possibly precessing, orbits is an important topic for future work. Moreover, the current method is highly compute-intensive. When the eccentricity becomes large, the convergence of the J-integrals slows markedly, and the overall cost of waveform generation grows almost exponentially. Developing more efficient algorithms to mitigate this scaling will thus be a key challenge for future work. In addition, one proof step in our tail-flux derivation remains open. We have not accounted for higher-order hereditary effects arising from couplings among multipole moments or from tail–memory interactions, nor have we incorporated radiation-reaction forces. Addressing these limitations will require further effort.

Acknowledgments

This work was supported in part by the National Key Research and Development Program of China Grant No. 2021YFC2203001 and in part by the NSFC (No. 12475046, No. 12021003 and No. 12005016). X. Liu is supported by the Consolidación Investigadora 2022 grant CNS2022-135211, the I+D grant PID2023-149018NB-C42, and the Grant IFT Centro de Excelencia Severo Ochoa No CEX2020-001007-S, funded by MCIN/AEI/10.13039/501100011033. Z.Cao was supported by “the Fundamental Research Funds for the Central Universities”.

4PN contact transformations

The conservative Lagrangian in SH coordinates depends not only on the positions and velocities of the component bodies, but also on their accelerations: $L(y^i, v^i, a^i)$, where y^i is the position and $v^i := \dot{y}^i, a^i := \dot{v}^i$. And the accelerations begin to appear from the 2PN order, and only the linear components of accelerations can be retained [102, 103]. Now the Lagrangian has already be derived in COM up to 4PN order [55, 56]. And the Lagrangian in ADM coordinates can be found in [58, 104, 105]. The accelerations and logarithmic terms can be canceled by applying a small contact transformation between SH and ADM [60],

$$y^i_{\mathrm{SH}} \to y^i_{\mathrm{ADM}} + \delta y^i_{\mathrm{SH}\to\mathrm{ADM}}(y^i_{\mathrm{ADM}}). \tag{140}$$

The difference δy starts at 2PN-order, we need to expand the variation of the Lagrangian up to $\mathcal{O}\big(\delta y^3\big)$,

$$\delta L := L(y^i + \delta y^i) - L(y^i) = \delta L^{(1)} + \frac{1}{2}\delta L^{(2)} + \mathcal{O}\big(\delta y^3\big), \tag{141}$$

where the $\mathcal{O}(\delta y)$ term reads

$$\delta L^{(1)} = \frac{\delta L}{\delta y^i}\delta y^i + \frac{\mathrm{d}Q^{(1)}}{\mathrm{d}t}, \tag{142}$$

$$\frac{\delta L}{\delta y^i} = L_{y^i} - \dot{L}_{v^i} + \ddot{L}_{a^i} \tag{143}$$

$$Q^{(1)} = (L_{v^i} - \dot{L}_{a^i})\delta y^i + L_{a^i}\delta v^i \tag{144}$$

We use the shorthands $L_Y := \partial L/\partial Y$, and $\delta v^i := \delta\dot{y}^i, \delta a^i := \delta\dot{v}^i$. The $\mathcal{O}\big(\delta y^2\big)$ term is

$$\delta L^{(2)} = \delta y^i \mathcal{J}^{ij}\delta y^j + \frac{\mathrm{d}Q^{(2)}}{\mathrm{d}t}, \tag{145}$$

$$\mathcal{J}^{ij} = L_{y^i y^j} - \frac{\mathrm{d}}{\mathrm{d}t}L_{v^i v^j}\frac{\mathrm{d}}{\mathrm{d}t} + \frac{\mathrm{d}^2}{\mathrm{d}t^2}L_{a^i a^j}\frac{\mathrm{d}^2}{\mathrm{d}t^2} - 2\frac{\mathrm{d}}{\mathrm{d}t}L_{v^i y^j} + 2\frac{\mathrm{d}^2}{\mathrm{d}t^2}L_{a^i y^j} + 2\frac{\mathrm{d}^2}{\mathrm{d}t^2}L_{a^i v^j}\frac{\mathrm{d}}{\mathrm{d}t}$$

$$\begin{aligned} Q^{(2)} &= L_{v^i v^j}\delta y^i \delta v^j + L_{a^i a^j}\delta v^i \delta a^j - \frac{\mathrm{d}}{\mathrm{d}t}\big(L_{a^i a^j}\delta a^j\big)\delta y^i + 2L_{v^i y^j}\delta y^i \delta y^j \\ &+ 2L_{a^i y^j}\delta v^i \delta y^j - 2\frac{\mathrm{d}}{\mathrm{d}t}\big(L_{a^i y^j}\delta y^j\big)\delta y^i + 2L_{a^i v^j}\delta v^i \delta v^j - 2\frac{\mathrm{d}}{\mathrm{d}t}\big(L_{a^i v^j}\delta v^j\big)\delta y^i. \end{aligned} \tag{146}$$

The transformation of Lagrangian is composed of two part,

$$L' = L + \frac{\mathrm{d}Q}{\mathrm{d}t} + \frac{\delta L}{\delta y^i}\delta y^i + \frac{1}{2}\delta y^i \mathcal{J}^{ij}\delta y^j + \mathcal{O}(\delta y^3), \tag{147}$$

We separate L into three parts,

$$L = L' + \delta L_{\mathrm{na}} + L_{a^i}a^i, \tag{148}$$

where δL_{na} denotes the different terms that don't involve acceleration. We can add any total-derivative term $\mathrm{d}F\,/\,\mathrm{d}t$ that don't affect the dynamics. One just need to make sure

$$0 = \delta L_{\mathrm{na}} + L_{a^i}a^i + F_{y^i}v^i + F_{v^i}a^i + F_{a^i}b^i + \frac{\delta L}{\delta y^i}\delta y^i + \frac{1}{2}\delta y^i \mathcal{J}^{ij}\delta y^j, \tag{149}$$

where $b^i := \dot{a}^i$. At the 4PN level we must introduce acceleration into F, finally we get

$$\begin{aligned}
\delta\boldsymbol{y}_{\mathrm{SH}\to\mathrm{ADM}} &= \frac{1}{c^4}\bigg[\bigg(-\frac{\nu\dot{r}^2}{8} + \Big(3\nu + \frac{1}{4}\Big)\frac{1}{r} + \frac{5\nu v^2}{8}\bigg)\hat{\boldsymbol{n}} - \frac{9\nu\dot{r}}{4}\boldsymbol{v}\bigg] + \frac{1}{c^6}\bigg\{\bigg[\frac{1}{r^2}\bigg(\frac{22}{3}\ln\Big(\frac{r}{r'_0}\Big) - \frac{21\pi^2}{32} - \frac{2773}{280}\bigg)\nu \\
&+ \Big(\frac{\nu}{16} - \frac{5\nu^2}{16}\Big)\dot{r}^4 + \Big(\frac{15\nu^2}{16} - \frac{5\nu}{16}\Big)\dot{r}^2v^2 + \frac{1}{r}\bigg(\Big(\frac{5\nu^2}{2} - \frac{161\nu}{48}\Big)\dot{r}^2 + \Big(\frac{3\nu^2}{8} + \frac{451\nu}{48}\Big)v^2\bigg) + \Big(\frac{\nu}{2} - \frac{11\nu^2}{8}\Big)v^4\bigg]\hat{\boldsymbol{n}} \\
&+ \bigg[\Big(\frac{5\nu}{12} - \frac{29\nu^2}{24}\Big)\dot{r}^3 + \frac{1}{r}\Big(-5\nu^2 - \frac{43\nu}{3}\Big)\dot{r} + \Big(\frac{21\nu^2}{4} - \frac{17\nu}{8}\Big)\dot{r}v^2\bigg]\boldsymbol{v}\bigg\} + \frac{1}{c^8}\bigg\{\bigg[\frac{49}{4}\nu^2\dot{r}a_v + \Big(-\frac{105\nu^3}{256} + \frac{35\nu^2}{128} - \frac{5\nu}{128}\Big)\dot{r}^6 \\
&+ \Big(-\frac{1143\nu^3}{256} + \frac{339\nu^2}{128} - \frac{53\nu}{128}\Big)\dot{r}^2v^4 + \Big(\frac{555\nu^3}{256} - \frac{181\nu^2}{128} + \frac{27\nu}{128}\Big)\dot{r}^4v^2 + \Big(\frac{1253\nu^3}{256} - \frac{361\nu^2}{128} + \frac{55\nu}{128}\Big)v^6 \\
&+ \frac{1}{r}\bigg(\frac{9}{32}\nu^2 r\dot{r}^2 a_r + v^2\bigg[\Big(-\frac{535\nu^3}{64} + \frac{10247\nu^2}{384} - \frac{341\nu}{40}\Big)\dot{r}^2 - \frac{171}{32}\nu^2 r a_r\bigg] + \Big(\frac{1337\nu^3}{384} - \frac{4765\nu^2}{256} + \frac{313\nu}{480}\Big)\dot{r}^4 \\
&+ \Big(-\frac{421\nu^3}{128} - \frac{18263\nu^2}{768} + \frac{2031\nu}{160}\Big)v^4\bigg) + \frac{1}{r^2}\bigg(\dot{r}^2\bigg[\nu^2\bigg(-11\ln\Big(\frac{r}{r'_0}\Big) + 44\ln\Big(\frac{r}{r''_0}\Big) - \frac{7449\pi^2}{16384} - \frac{1312259}{134400}\bigg) \\
&+ \bigg(-11\ln\Big(\frac{r}{r''_0}\Big) - \frac{10119\pi^2}{8192} - \frac{3629869}{44800}\bigg)\nu + \frac{71\nu^3}{8}\bigg] + v^2\bigg[\bigg(22\ln\Big(\frac{r}{r'_0}\Big) - \frac{6629\pi^2}{8192} + \frac{9427}{256}\bigg)\nu + \frac{\nu^3}{8} \\
&+ \Big(-\frac{439447}{57600} - \frac{18107\pi^2}{16384}\Big)\nu^2\bigg]\bigg) + \frac{1}{r^3}\bigg(\nu^2\bigg[-120\ln\Big(\frac{r}{r'_0}\Big) + 240\ln\Big(\frac{r}{r''_0}\Big) - \frac{26389\pi^2}{3072} + \frac{3439}{144}\bigg] \\
&+ \nu\bigg(\frac{104}{3}\ln\Big(\frac{r}{r'_0}\Big) - 124\ln\Big(\frac{r}{r''_0}\Big) + \frac{8925\pi^2}{1024} - \frac{27169}{1440}\bigg) - 16\ln\Big(\frac{r}{r'_0}\Big) + 16\ln\Big(\frac{r}{r''_0}\Big)\bigg)\bigg]\hat{\boldsymbol{n}} + \bigg[-\frac{115\nu^2 a_v}{32} \\
&+ \Big(-\frac{121\nu^3}{128} + \frac{63\nu^2}{64} - \frac{13\nu}{64}\Big)\dot{r}^5 + \Big(-\frac{2449\nu^3}{128} + \frac{789\nu^2}{64} - \frac{135\nu}{64}\Big)\dot{r}v^4 + \Big(\frac{1193\nu^3}{192} - \frac{431\nu^2}{96} + \frac{77\nu}{96}\Big)\dot{r}^3v^2 \\
&+ \frac{1}{r}\bigg(\Big(-\frac{85\nu^3}{32} - \frac{615\nu^2}{64} + \frac{6737\nu}{480}\Big)\dot{r}^3 + \Big(\frac{803\nu^3}{32} + \frac{4199\nu^2}{192} - \frac{4851\nu}{160}\Big)\dot{r}v^2\bigg) + \frac{\dot{r}}{r^2}\bigg(\nu^2\bigg(\frac{44}{3}\ln\Big(\frac{r}{r'_0}\Big) - \frac{88}{3}\ln\Big(\frac{r}{r''_0}\Big) \\
&- \frac{28603\pi^2}{8192} + \frac{4066291}{201600}\bigg) + \nu\bigg(-44\ln\Big(\frac{r}{r'_0}\Big) + \frac{22}{3}\ln\Big(\frac{r}{r''_0}\Big) - \frac{1253\pi^2}{4096} + \frac{22800709}{201600}\bigg) - \frac{21\nu^3}{2}\bigg)\bigg]\boldsymbol{v}\bigg\} + \mathcal{O}(c^{-10}).
\end{aligned} \tag{150}$$

It is equivalent to [106]. Similarly,

$$\begin{aligned}
\delta\boldsymbol{y}_{\mathrm{SH}\to\mathrm{MH}} &= \frac{22\nu}{3r^2c^6}\ln\Big(\frac{r}{r'_0}\Big)\hat{\boldsymbol{n}} + \frac{1}{r^2c^8}\bigg\{\bigg[\dot{r}^2\bigg(\nu^2(44\ln\Big(\frac{r}{r''_0}\Big) - 11\ln\Big(\frac{r}{r'_0}\Big)) - 11\ln\Big(\frac{r}{r''_0}\Big)\nu\bigg) + 22\ln\Big(\frac{r}{r'_0}\Big)\nu v^2 \\
&+ \frac{1}{r}\bigg(\nu^2\bigg(240\ln\Big(\frac{r}{r''_0}\Big) - 120\ln\Big(\frac{r}{r'_0}\Big)\bigg) + \nu\bigg(\frac{104}{3}\ln\Big(\frac{r}{r'_0}\Big) - 124\ln\Big(\frac{r}{r''_0}\Big)\bigg) - 16\ln\Big(\frac{r}{r'_0}\Big) + 16\ln\Big(\frac{r}{r''_0}\Big)\bigg)\bigg]\hat{\boldsymbol{n}} \\
&+ \frac{\dot{r}}{r^2}\bigg(\nu^2\bigg(\frac{44}{3}\ln\Big(\frac{r}{r'_0}\Big) - \frac{88}{3}\ln\Big(\frac{r}{r''_0}\Big)\bigg) + \nu\bigg(\frac{22}{3}\ln\Big(\frac{r}{r''_0}\Big) - 44\ln\Big(\frac{r}{r'_0}\Big)\bigg)\bigg)\boldsymbol{v}\bigg\} + \mathcal{O}(c^{-10}).
\end{aligned} \tag{151}$$

[1] B. Abbott, R. Abbott, T. Abbott, M. Abernathy, F. Acernese, K. Ackley, C. Adams, T. Adams, P. Addesso, R. Adhikari, et al., Physical Review Letters **116** (2016), ISSN 1079-7114, URL `http://dx.doi.org/10.1103/PhysRevLett.116.061102`.

[2] T. L. S. Collaboration, J. Aasi, B. P. Abbott, R. Abbott, T. Abbott, M. R. Abernathy, K. Ackley, C. Adams, T. Adams, P. Addesso, et al., Classical and Quantum Gravity **32**, 074001 (2015), URL `https://dx.doi.org/10.1088/0264-9381/32/7/074001`.

[3] F. Acernese, M. Agathos, K. Agatsuma, D. Aisa, N. Allemandou, A. Allocca, J. Amarni, P. Astone, G. Balestri, G. Ballardin, et al., Classical and Quantum Gravity **32**, 024001 (2014), URL `https://dx.doi.org/10.1088/0264-9381/32/2/024001`.

[4] T. Akutsu, M. Ando, K. Arai, Y. Arai, S. Araki, A. Araya, N. Aritomi, Y. Aso, S. Bae, Y. Bae, et al., Progress of Theoretical and Experimental Physics **2021**, 05A101 (2020), ISSN 2050-3911, https://academic.oup.com/ptep/article-pdf/2021/5/05A101/37974994/ptaa125.pdf, URL `https://doi.org/10.1093/ptep/ptaa125`.

[5] LIGO, *Gwtc-2 data release documentation*, URL `https://www.gw-openscience.org/GWTC-2/`.

[6] The LIGO Scientific Collaboration, The Virgo Collaboration, The KAGRA Collaboration, R. Abbott, T. D. Abbott, F. Acernese, K. Ackley, C. Adams, N. Adhikari, R. X. Adhikari, et al. (2021).

[7] G. Agazie, A. Anumarlapudi, A. M. Archibald, Z. Arzoumanian, P. T. Baker, B. Bécsy, L. Blecha, A. Brazier, P. R. Brook, S. Burke-Spolaor, et al., The Astrophysical Journal Letters **951**, L8 (2023), ISSN 2041-8213, URL `http://dx.doi.org/10.3847/2041-8213/acdac6`.

[8] D. J. Reardon, A. Zic, R. M. Shannon, G. B. Hobbs, M. Bailes, V. Di Marco, A. Kapur, A. F. Rogers, E. Thrane, J. Askew, et al., The Astrophysical Journal Letters **951**, L6 (2023), ISSN 2041-8213, URL `http://dx.doi.org/10.3847/2041-8213/acdd02`.

[9] J. Antoniadis, P. Arumugam, S. Arumugam, S. Babak, M. Bagchi, A.-S. Bak Nielsen, C. G. Bassa, A. Bathula, A. Berthereau, M. Bonetti, et al., Astronomy amp; Astrophysics **678**, A50 (2023), ISSN 1432-0746, URL `http://dx.doi.org/10.1051/0004-6361/202346844`.

[10] H. Xu, S. Chen, Y. Guo, J. Jiang, B. Wang, J. Xu, Z. Xue, R. Nicolas Caballero, J. Yuan, Y. Xu, et al., Research in Astronomy and Astrophysics **23**, 075024 (2023), ISSN 1674-4527, URL `http://dx.doi.org/10.1088/1674-4527/acdfa5`.

[11] M. Punturo, M. Abernathy, F. Acernese, B. Allen, N. Andersson, K. Arun, F. Barone, B. Barr, M. Barsuglia, M. Beker, et al., Classical and Quantum Gravity **27**, 194002 (2010), URL `https://iopscience.iop.org/article/10.1088/0264-9381/27/19/194002`.

[12] M. Evans, R. X. Adhikari, C. Afle, S. W. Ballmer, S. Biscoveanu, S. Borhanian, D. A. Brown, Y. Chen, R. Eisenstein, A. Gruson, et al., *A horizon study for cosmic explorer: Science, observatories, and community* (2021), 2109.09882.

[13] K. D. for the LISA Study Team, Classical and Quantum Gravity **14**, 1399 (1997), URL `https://iopscience.iop.org/article/10.1088/0264-9381/14/6/002`.

[14] J. Luo, L.-S. Chen, H.-Z. Duan, Y.-G. Gong, S. Hu, J. Ji, Q. Liu, J. Mei, V. Milyukov, M. Sazhin, et al., Classical and Quantum Gravity **33**, 035010 (2016), ISSN 1361-6382, URL `http://dx.doi.org/10.1088/0264-9381/33/3/035010`.

[15] W.-H. Ruan, Z.-K. Guo, R.-G. Cai, and Y.-Z. Zhang, International Journal of Modern Physics A **35**, 2050075 (2020), ISSN 1793-656X, URL `http://dx.doi.org/10.1142/S0217751X2050075X`.

[16] S. Kawamura et al., Class. Quant. Grav. **23**, S125 (2006).

[17] G. Landini and A. Strumia, *Optical gravitational waves as signals of gravitationally-decaying particles* (2025), 2501.09794, URL `https://arxiv.org/abs/2501.09794`.

[18] D. George and E. Huerta, Physical Review D **97** (2018), ISSN 2470-0029, URL `http://dx.doi.org/10.1103/PhysRevD.97.044039`.

[19] M. Boyle, D. Hemberger, D. A. B. Iozzo, G. Lovelace, S. Ossokine, H. P. Pfeiffer, M. A. Scheel, L. C. Stein, C. J. Woodford, A. B. Zimmerman, et al., Classical and Quantum Gravity **36**, 195006 (2019), ISSN 1361-6382, URL `http://dx.doi.org/10.1088/1361-6382/ab34e2`.

[20] E. Hamilton, E. Fauchon-Jones, M. Hannam, C. Hoy, C. Kalaghatgi, L. London, J. E. Thompson, D. Yeeles, S. Ghosh, S. Khan, et al., *A catalogue of precessing black-hole-binary numerical-relativity simulations* (2023), 2303.05419, URL `https://arxiv.org/abs/2303.05419`.

[21] M. A. Scheel, M. Boyle, K. Mitman, N. Deppe, L. C. Stein, C. Armaza, M. S. Bonilla, L. T. Buchman, A. Ceja, H. Chaudhary, et al., *The sxs collaboration's third catalog of binary black hole simulations* (2025), 2505.13378, URL `https://arxiv.org/abs/2505.13378`.

[22] Y. Mino, M. Sasaki, and T. Tanaka, Physical Review D **55**, 3457–3476 (1997), ISSN 1089-4918, URL `http://dx.doi.org/10.1103/PhysRevD.55.3457`.

[23] A. Pound, Physical Review Letters **109** (2012), ISSN 1079-7114, URL `http://dx.doi.org/10.1103/PhysRevLett.109.051101`.

[24] L. Blanchet, *Post-newtonian theory for gravitational waves* (2024), 1310.1528, URL `https://arxiv.org/abs/1310.1528`.

[25] A. Buonanno and T. Damour, Physical Review D **59** (1999), ISSN 1089-4918, URL `http://dx.doi.org/10.1103/PhysRevD.59.084006`.

[26] Y. Pan, A. Buonanno, M. Boyle, L. T. Buchman, L. E. Kidder, H. P. Pfeiffer, and M. A. Scheel, Physical Review D **84** (2011), ISSN 1550-2368, URL `http://dx.doi.org/10.1103/PhysRevD.84.124052`.

[27] A. Bohé, L. Shao, A. Taracchini, A. Buonanno, S. Babak, I. W. Harry, I. Hinder, S. Ossokine, M. Pürrer, V. Raymond,

et al., Physical Review D **95** (2017), ISSN 2470-0029, URL http://dx.doi.org/10.1103/PhysRevD.95.044028.
[28] Z. Cao and W.-B. Han, Phys. Rev. D **96**, 044028 (2017), URL https://link.aps.org/doi/10.1103/PhysRevD.96.044028.
[29] X. Liu, Z. Cao, and Z.-H. Zhu, Classical and Quantum Gravity **41**, 195019 (2024).
[30] A. Gamboa, M. Khalil, and A. Buonanno, *Third post-newtonian dynamics for eccentric orbits and aligned spins in the effective-one-body waveform model seobnrv5ehm* (2024), 2412.12831, URL https://arxiv.org/abs/2412.12831.
[31] H. Estellés, A. Buonanno, R. Enficiaud, C. Foo, and L. Pompili, *Adding equatorial-asymmetric effects for spin-precessing binaries into the seobnrv5phm waveform model* (2025), 2506.19911, URL https://arxiv.org/abs/2506.19911.
[32] A. Nagar, S. Bernuzzi, W. Del Pozzo, G. Riemenschneider, S. Akcay, G. Carullo, P. Fleig, S. Babak, K. W. Tsang, M. Colleoni, et al., Physical Review D **98** (2018), ISSN 2470-0029, URL http://dx.doi.org/10.1103/PhysRevD.98.104052.
[33] S. Akcay, R. Gamba, and S. Bernuzzi, Physical Review D **103** (2021), ISSN 2470-0029, URL http://dx.doi.org/10.1103/PhysRevD.103.024014.
[34] A. Nagar, R. Gamba, P. Rettegno, V. Fantini, and S. Bernuzzi, *Effective-one-body waveform model for non-circularized, planar, coalescing black hole binaries: the importance of radiation reaction* (2024), 2404.05288, URL https://arxiv.org/abs/2404.05288.
[35] P. Ajith et al., I: Non-spinning binaries (2007).
[36] P. Ajith, M. Hannam, S. Husa, Y. Chen, B. Brügmann, N. Dorband, D. Müller, F. Ohme, D. Pollney, C. Reisswig, et al., Physical Review Letters **106** (2011), ISSN 1079-7114, URL http://dx.doi.org/10.1103/PhysRevLett.106.241101.
[37] S. Khan, S. Husa, M. Hannam, F. Ohme, M. Pürrer, X. J. Forteza, and A. Bohé, Physical Review D **93** (2016), ISSN 2470-0029, URL http://dx.doi.org/10.1103/PhysRevD.93.044007.
[38] L. London, S. Khan, E. Fauchon-Jones, C. García, M. Hannam, S. Husa, X. Jiménez-Forteza, C. Kalaghatgi, F. Ohme, and F. Pannarale, Physical Review Letters **120** (2018), ISSN 1079-7114, URL http://dx.doi.org/10.1103/PhysRevLett.120.161102.
[39] C. García-Quirós, M. Colleoni, S. Husa, H. Estellés, G. Pratten, A. Ramos-Buades, M. Mateu-Lucena, and R. Jaume, Physical Review D **102** (2020), ISSN 2470-0029, URL http://dx.doi.org/10.1103/PhysRevD.102.064002.
[40] P. Manna, T. RoyChowdhury, and C. K. Mishra, Physical Review D **111** (2025), ISSN 2470-0029, URL http://dx.doi.org/10.1103/849s-3zy8.
[41] M. de Lluc Planas, A. Ramos-Buades, C. García-Quirós, H. Estellés, S. Husa, and M. Haney, *Time-domain phenomenological multipolar waveforms for aligned-spin binary black holes in elliptical orbits* (2025), 2503.13062, URL https://arxiv.org/abs/2503.13062.
[42] R. Abbott, T. Abbott, S. Abraham, F. Acernese, K. Ackley, C. Adams, R. Adhikari, V. Adya, C. Affeldt, M. Agathos, et al., Physical Review Letters **125** (2020), ISSN 1079-7114, URL http://dx.doi.org/10.1103/PhysRevLett.125.101102.
[43] T. Damour and N. Deruelle, Annales de l'I.H.P. Physique théorique **43**, 107 (1985), URL https://www.numdam.org/item/AIHPA_1985__43_1_107_0/.
[44] T. Damour and G. Schäeer, Il Nuovo Cimento B (1971-1996) **101**, 127 (1988).
[45] G. Schäfer and N. Wex, Physics Letters A **174**, 196 (1993).
[46] R.-M. Memmesheimer, A. Gopakumar, and G. Schäfer, Phys. Rev. D **70**, 104011 (2004), URL https://link.aps.org/doi/10.1103/PhysRevD.70.104011.
[47] A. Pound and E. Poisson, Physical Review D **77** (2008), ISSN 1550-2368, URL http://dx.doi.org/10.1103/PhysRevD.77.044012.
[48] J. Miller and A. Pound, Physical Review D **103** (2021), ISSN 2470-0029, URL http://dx.doi.org/10.1103/PhysRevD.103.064048.
[49] N. Yunes, K. G. Arun, E. Berti, and C. M. Will, Physical Review D **80** (2009), ISSN 1550-2368, URL http://dx.doi.org/10.1103/PhysRevD.80.084001.
[50] A. Klein, N. Cornish, and N. Yunes, Physical Review D **88** (2013), ISSN 1550-2368, URL http://dx.doi.org/10.1103/PhysRevD.88.124015.
[51] G. Morras, G. Pratten, and P. Schmidt, Physical Review D **111** (2025), ISSN 2470-0029, URL http://dx.doi.org/10.1103/PhysRevD.111.084052.
[52] K. G. Arun, L. Blanchet, B. R. Iyer, and M. S. S. Qusailah, Physical Review D **77** (2008), ISSN 1550-2368, URL http://dx.doi.org/10.1103/PhysRevD.77.064034.
[53] G. Morras, *Modeling gravitational wave modes from binaries with arbitrary eccentricity* (2025), 2507.00169, URL https://arxiv.org/abs/2507.00169.
[54] D. Thibault and S. Gerhard, General Relativity and Gravitation **17** (1085), ISSN 1572-9532, URL https://doi.org/10.1007/BF00773685.
[55] L. Bernard, L. Blanchet, A. Bohé, G. Faye, and S. Marsat, Phys. Rev. D **93**, 084037 (2016), URL https://link.aps.org/doi/10.1103/PhysRevD.93.084037.
[56] L. Bernard, L. Blanchet, G. Faye, and T. Marchand, Phys. Rev. D **97**, 044037 (2018), URL https://link.aps.org/doi/10.1103/PhysRevD.97.044037.
[57] L. Blanchet and T. Damour, Phys. Rev. D **37**, 1410 (1988), URL https://link.aps.org/doi/10.1103/PhysRevD.37.1410.
[58] T. Damour, P. Jaranowski, and G. Schäfer, Phys. Rev. D **89**, 064058 (2014), URL https://link.aps.org/doi/10.1103/PhysRevD.89.064058.

[59] L. Blanchet and G. Faye, Journal of Mathematical Physics **41**, 7675–7714 (2000), ISSN 1089-7658, URL `http://dx.doi.org/10.1063/1.1308506`.
[60] V. C. d. Andrade, L. Blanchet, and G. Faye, Classical and Quantum Gravity **18**, 753–778 (2001), ISSN 1361-6382, URL `http://dx.doi.org/10.1088/0264-9381/18/5/301`.
[61] L. Blanchet, B. R. Iyer, and B. Joguet, Phys. Rev. D **65**, 064005 (2002), URL `https://link.aps.org/doi/10.1103/PhysRevD.65.064005`.
[62] I. Hinder, F. Herrmann, P. Laguna, and D. Shoemaker, Physical Review D **82** (2010), ISSN 1550-2368, URL `http://dx.doi.org/10.1103/PhysRevD.82.024033`.
[63] E. Huerta, P. Kumar, S. T. McWilliams, R. O'Shaughnessy, and N. Yunes, Physical Review D **90** (2014), ISSN 1550-2368, URL `http://dx.doi.org/10.1103/PhysRevD.90.084016`.
[64] B. Moore, M. Favata, K. Arun, and C. K. Mishra, Physical Review D **93** (2016), ISSN 2470-0029, URL `http://dx.doi.org/10.1103/PhysRevD.93.124061`.
[65] A. Klein, Y. Boetzel, A. Gopakumar, P. Jetzer, and L. de Vittori, Physical Review D **98** (2018), ISSN 2470-0029, URL `http://dx.doi.org/10.1103/PhysRevD.98.104043`.
[66] G. Cho, S. Tanay, A. Gopakumar, and H. M. Lee, Physical Review D **105** (2022), ISSN 2470-0029, URL `http://dx.doi.org/10.1103/PhysRevD.105.064010`.
[67] T. Damour, P. Jaranowski, and G. Schäfer, Physical Review D **91** (2015), ISSN 1550-2368, URL `http://dx.doi.org/10.1103/PhysRevD.91.084024`.
[68] D. Bini, T. Damour, and A. Geralico, Physical Review D **102** (2020), ISSN 2470-0029, URL `http://dx.doi.org/10.1103/PhysRevD.102.024062`.
[69] M. Khalil, A. Buonanno, H. Estellés, D. P. Mihaylov, S. Ossokine, L. Pompili, and A. Ramos-Buades, *Theoretical groundwork supporting the precessing-spin two-body dynamics of the effective-one-body waveform models seobnrv5* (2023), 2303.18143, URL `https://arxiv.org/abs/2303.18143`.
[70] Y. Boetzel, A. Susobhanan, A. Gopakumar, A. Klein, and P. Jetzer, Phys. Rev. D **96**, 044011 (2017), URL `https://link.aps.org/doi/10.1103/PhysRevD.96.044011`.
[71] K. S. Thorne, Rev. Mod. Phys. **52**, 299 (1980), URL `https://link.aps.org/doi/10.1103/RevModPhys.52.299`.
[72] L. Blanchet and T. Damour, Philosophical transactions of the royal society of London. Series a, mathematical and physical sciences **320**, 379 (1986).
[73] L. Blanchet, Classical and Quantum Gravity **15**, 1971–1999 (1998), ISSN 1361-6382, URL `http://dx.doi.org/10.1088/0264-9381/15/7/013`.
[74] D. Bini and T. Damour, Physical Review D **86** (2012), ISSN 1550-2368, URL `http://dx.doi.org/10.1103/PhysRevD.86.124012`.
[75] G. Fumagalli, N. Loutrel, D. Gerosa, and M. Boschini, Physical Review D **112** (2025), ISSN 2470-0029, URL `http://dx.doi.org/10.1103/znmj-6wvt`.
[76] (????).
[77] A. Gopakumar, B. R. Iyer, and S. Iyer, Phys. Rev. D **55**, 6030 (1997), URL `https://link.aps.org/doi/10.1103/PhysRevD.55.6030`.
[78] A. K. Leibovich, B. A. Pardo, and Z. Yang, Physical Review D **108** (2023), ISSN 2470-0029, URL `http://dx.doi.org/10.1103/PhysRevD.108.024017`.
[79] L. Blanchet, G. Faye, and D. Trestini, *Gravitational radiation reaction for compact binary systems at the fourth-and-a-half post-newtonian order* (2024), 2407.18295, URL `https://arxiv.org/abs/2407.18295`.
[80] C. Königsdörffer and A. Gopakumar, Physical Review D **73** (2006), ISSN 1550-2368, URL `http://dx.doi.org/10.1103/PhysRevD.73.124012`.
[81] S. Tiwari and A. Gopakumar, Physical Review D **102** (2020), ISSN 2470-0029, URL `http://dx.doi.org/10.1103/PhysRevD.102.084042`.
[82] B. Mikóczi, P. Forgács, and M. Vasúth, Physical Review D **92** (2015), ISSN 1550-2368, URL `http://dx.doi.org/10.1103/PhysRevD.92.044038`.
[83] C. Munna and C. R. Evans, Physical Review D **102** (2020), ISSN 2470-0029, URL `http://dx.doi.org/10.1103/PhysRevD.102.104006`.
[84] C. Munna and C. R. Evans, Physical Review D **106** (2022), ISSN 2470-0029, URL `http://dx.doi.org/10.1103/PhysRevD.106.044004`.
[85] D. Trestini, Classical and Quantum Gravity **42**, 155016 (2025), ISSN 1361-6382, URL `http://dx.doi.org/10.1088/1361-6382/adedf5`.
[86] P. C. Peters, Phys. Rev. **136**, B1224 (1964), URL `https://link.aps.org/doi/10.1103/PhysRev.136.B1224`.
[87] A. V. Gerhard Beutler, Leos Mervart, *Methods of celestial mechanics Volume 1*, Astronomy and astrophysics library (Springer, 2005), 1st ed., ISBN 3540407499; 9783540407492; 3540407502; 9783540407508.
[88] M. K. Kazuhiko Aomoto, *Theory of Hypergeometric Functions* (Springer Tokyo, 2011), 1st ed., URL `https://doi.org/10.1007/978-4-431-53938-4`.
[89] G. N. Watson, *A Treatise on the Theory of Bessel Functions*, Cambridge Mathematical Library (Cambridge, 1995), 2nd ed., ISBN 9780521483919.
[90] K. G. Arun, L. Blanchet, B. R. Iyer, and M. S. S. Qusailah, Physical Review D **77** (2008), ISSN 1550-2368, URL `http://dx.doi.org/10.1103/PhysRevD.77.064035`.
[91] C. K. Mishra, K. Arun, and B. R. Iyer, Physical Review D **91** (2015), ISSN 1550-2368, URL `http://dx.doi.org/10.1103/PhysRevD.91.084040`.

[92] T. Marchand, Q. Henry, F. Larrouturou, S. Marsat, G. Faye, and L. Blanchet, Classical and Quantum Gravity **37**, 215006 (2020), ISSN 1361-6382, URL `http://dx.doi.org/10.1088/1361-6382/ab9ce1`.

[93] L. Blanchet, G. Faye, B. R. Iyer, and S. Sinha, Classical and Quantum Gravity **25**, 165003 (2008), ISSN 1361-6382, URL `http://dx.doi.org/10.1088/0264-9381/25/16/165003`.

[94] N. Loutrel and N. Yunes, Classical and Quantum Gravity **34**, 044003 (2017), ISSN 1361-6382, URL `http://dx.doi.org/10.1088/1361-6382/aa59c3`.

[95] F. G. Ledesma and M. Mewes, Physical Review Research **2** (2020), ISSN 2643-1564, URL `http://dx.doi.org/10.1103/PhysRevResearch.2.043061`.

[96] Y. Boetzel, C. K. Mishra, G. Faye, A. Gopakumar, and B. R. Iyer, Physical Review D **100** (2019), ISSN 2470-0029, URL `http://dx.doi.org/10.1103/PhysRevD.100.044018`.

[97] D. Trestini and L. Blanchet, Physical Review D **107** (2023), ISSN 2470-0029, URL `http://dx.doi.org/10.1103/PhysRevD.107.104048`.

[98] L. Blanchet, G. Faye, Q. Henry, F. Larrouturou, and D. Trestini, Physical Review D **108** (2023), ISSN 2470-0029, URL `http://dx.doi.org/10.1103/PhysRevD.108.064041`.

[99] T. Marchand, L. Blanchet, and G. Faye, Classical and Quantum Gravity **33**, 244003 (2016), ISSN 1361-6382, URL `http://dx.doi.org/10.1088/0264-9381/33/24/244003`.

[100] D. Trestini, Physical Review D **112** (2025), ISSN 2470-0029, URL `http://dx.doi.org/10.1103/lsbb-sv45`.

[101] K. Arun, L. Blanchet, B. Iyer, and S. Sinha, Physical Review D **80** (2009), ISSN 1550-2368, URL `http://dx.doi.org/10.1103/PhysRevD.80.124018`.

[102] T. Damour and N. Deruelle, Comptes Rendus des Seances de l'Academie des Sciences. Serie 2 **293**, 537 (1981).

[103] T. Damour and G. Schaefer, J. Math. Phys. **32**, 127 (1991).

[104] P. Jaranowski and G. Schäfer, Physical Review D **87** (2013), ISSN 1550-2368, URL `http://dx.doi.org/10.1103/PhysRevD.87.081503`.

[105] P. Jaranowski and G. Schäfer, Physical Review D **92** (2015), ISSN 1550-2368, URL `http://dx.doi.org/10.1103/PhysRevD.92.124043`.

[106] L. Blanchet, D. Langlois, and E. Ligout, *Innermost stable circular orbit of arbitrary-mass compact binaries at fourth post-newtonian order* (2025), 2505.01278, URL `https://arxiv.org/abs/2505.01278`.